




Low-accommodation and backwater effects on sequence stratigraphic surfaces and depositional architecture of fluvio-deltaic settings (Cretaceous Mesa Rica Sandstone, Dakota Group, USA)

Anna E. van Yperen¹  | John M. Holbrook² | Miquel Poyatos-Moré¹  |
Cody Myers^{2,3} | Ivar Midtkandal¹ 

¹Department of Geosciences, University of Oslo, Oslo, Norway

²Department of Geological Sciences, Texas Christian University, Fort Worth, TX, USA

³Pagosa Outside Adventures, Pagosa Springs, TX, USA

Correspondence

Anna E. van Yperen, Department of Geosciences, University of Oslo, P.O. Box 1047 Blindern, 0316 Oslo, Norway.
Email: annavanyperen@gmail.com

Funding information

Research Centre for Arctic Petroleum Exploration (ARCEX); Lower Cretaceous basinal studies of the Arctic (LoCra)

Abstract

The adequate documentation and interpretation of regional-scale stratigraphic surfaces is paramount to establish correlations between continental and shallow marine strata. However, this is often challenged by the amalgamated nature of low-accommodation settings and control of backwater hydraulics on fluvio-deltaic stratigraphy. Exhumed examples of full-transect depositional profiles across river-to-delta systems are key to improve our understanding about interacting controlling factors and resultant stratigraphy. This study utilizes the ~400 km transect of the Cenomanian Mesa Rica Sandstone (Dakota Group, USA), which allows mapping of down-dip changes in facies, thickness distribution, fluvial architecture and spatial extent of stratigraphic surfaces. The two sandstone units of the Mesa Rica Sandstone represent contemporaneous fluvio-deltaic deposition in the Tucumcari sub-basin (Western Interior Basin) during two regressive phases. Multivalley deposits pass down-dip into single-story channel sandstones and eventually into contemporaneous distributary channels and delta-front strata. Down-dip changes reflect accommodation decrease towards the paleoshoreline at the Tucumcari basin rim, and subsequent expansion into the basin. Additionally, multi-storey channel deposits bound by erosional composite scours incise into underlying deltaic deposits. These represent incised-valley fill deposits, based on their regional occurrence, estimated channel tops below the surrounding topographic surface and coeval downstepping delta-front geometries. This opposes criteria offered to differentiate incised valleys from flood-induced backwater scours. As the incised valleys evidence relative sea-level fall and flood-induced backwater scours do not, the interpretation of incised valleys impacts sequence stratigraphic interpretations. The erosional composite surface below fluvial strata in the continental realm represents a sequence boundary/regional composite

The peer review history for this article is available at <https://publons.com/publon/10.1111/bre.12483>.

This is an open access article under the terms of the Creative Commons Attribution License, which permits use, distribution and reproduction in any medium, provided the original work is properly cited.

© 2020 The Authors. Basin Research published by International Association of Sedimentologists and European Association of Geoscientists and Engineers and John Wiley & Sons Ltd

scour (RCS). The RCS' diachronous nature demonstrates that its down-dip equivalent disperses into several surfaces in the marine part of the depositional system, which challenges the idea of a single, correlatable surface. Formation of a regional composite scour in the fluvial realm throughout a relative sea-level cycle highlights that erosion and deposition occur virtually contemporaneously at any point along the depositional profile. This contradicts stratigraphic models that interpret low-accommodation settings to dominantly promote bypass, especially during forced regressions. Source-to-sink analyses should account for this in order to adequately resolve timing and volume of sediment storage in the system throughout a complete relative sea-level cycle.

KEYWORDS

backwater, fluvio-deltaic, full transect, low accommodation, sequence stratigraphy

1 | INTRODUCTION

The study of regional transects along depositional profiles is essential to establish robust sequence stratigraphic frameworks, which allow reconstructing the evolution of sedimentary basins (Amorosi, Maselli, & Trincardi, 2016; Bhattacharya, 2011; Blum, Martin, Milliken, & Garvin, 2013; Pattison, 2019; Van Wagoner, 1995). However, complete preservation of such large-scale profiles is rare, especially in low-accommodation settings (Ainsworth et al., 2017; Korus & Fielding, 2017). Low-accommodation systems tend to promote lateral rather than vertical stacking, and successions often equal the thickness of the main building block or architectural element (i.e. channel/ mouth bar; e.g. Ainsworth et al., 2017; Holbrook, 2001). The amalgamated nature of resulting deposits challenges the analysis of depositional architecture, and decreases the chances of key stratigraphic surfaces to be well-preserved. One of these surfaces is the sequence boundary, which has been proven composite and diachronous by flume and field observations (Bhattacharya, 2011; Hodgson, Kane, Flint, Brunt, & Ortiz-Karpf, 2016; Holbrook & Bhattacharya, 2012; Madof, Harris, & Connell, 2016; Martin, Paola, Abreu, Neal, & Sheets, 2009; Strong & Paola, 2008; Zuchuat et al., 2019). This has led to the introduction of the *Regional Composite Scour* (RCS; sensu Holbrook & Bhattacharya, 2012), as the component of the sequence boundary that results from multi-phase fluvial scours shaped throughout a relative sea-level cycle (e.g. Blum et al., 2013; Holbrook & Bhattacharya, 2012; Martin et al., 2009; Strong & Paola, 2008). Such a diachronous unconformity further complicates the correlation between coastal and shallow marine strata (Bhattacharya, 2011; Bhattacharya, Miall et al., 2019), but the concept is yet to be applied to low-accommodation systems.

The river graded stream profile has a natural tendency to re-establish equilibrium, and changes over time when influenced by variations in upstream and/or downstream allogenic

Highlights

- Exhumed ~400 km river-to-delta transect along a depositional dip-parallel profile.
- Laterally extensive sand-prone strata throughout the study area characterize deposition in a low-accommodation setting.
- Incised valley scours resulted from steepening of the graded stream profile and not as a consequence of flood-induced scouring in the backwater zone.
- The down-dip extension of the sequence boundary into marine realm consists of several dispersed surfaces.

factors (e.g. climate, tectonics, sea level). This can culminate in a spectrum of possible profiles (Bagnold, 1977; Hack, 1973; Mackin, 1948; Quirk, 1996; Snow & Slingerland, 1987). The lower- and uppermost possible profiles resemble the lowest level to which a stream may erode, and the highest level to which it may aggrade, respectively, and the space between these dictates accommodation (Figure 1b; Holbrook, Scott, & Oboh-Ikuenobe, 2006). The two profiles diverge in upstream direction (Bagnold, 1977; Hack, 1973; Mackin, 1948; Snow & Slingerland, 1987) and converge downstream towards base level (i.e. sea level), where fluvial accommodation is lowest (Figure 1b; Holbrook et al., 2006).

The river bed profile is also influenced by the receiving body of marine water in the downstream part of a fluvio-deltaic system, (e.g. Chow, 1959; Nittrouer, Shaw, Lamb, & Mohrig, 2012). The landward limit of this marine influence marks the upstream boundary of the backwater zone, defined as the reach where the river bed drops below sea level (Figure 1b). Its length depends on the bankfull channel depth and water-surface slope (Paola & Mohrig, 1996). In

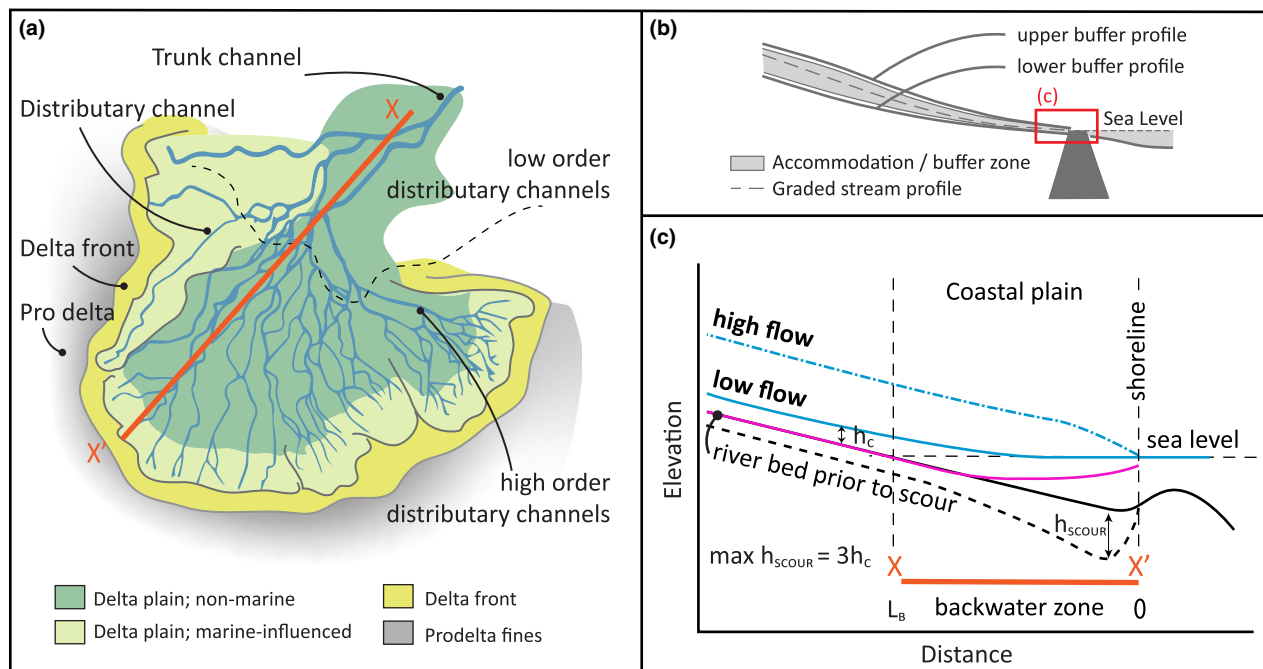


FIGURE 1 (a) Schematic drawing of a delta plain which illustrates frequently used terms in the paper. Lower order distributary channels include distributary channels with 1–3 successive bifurcations. (b) Projection of (c) onto graded stream profile and enveloping accommodation. The upper and lower buffer profiles track the highest surface of aggradation and the lowest depth of incision, respectively. These profiles converge towards sea level (modified from Holbrook et al., 2006). (c) Scheme for predicted scour patterns in the backwater zone under variable flow conditions. Averaged river bed elevation prior to scouring (solid lines) or after backwater induced scouring (dashed line). L_b = backwater length, h_c = bankfull flow depth, h_{scour} = maximum scour depth (modified from Trower et al., 2018). Pink solid line is inferred from Blum et al. (2013, Figure 4)

low-gradient river systems, backwater effects can extend for tens to hundreds of kilometres upstream (Blum et al., 2013). Recent studies have discussed the potential control of backwater hydraulics on discharge variations and resulting sedimentary architecture in the backwater zone (Blum et al., 2013; Chatanantavet & Lamb, 2014; Chatanantavet, Lamb, & Nittrouer, 2012; Colombara, Shiers, & Mountney, 2016; Fernandes, Törnqvist, Straub, & Mohrig, 2016; Ganti, Lamb, & Chadwick, 2019; Gugliotta & Saito, 2019; Lamb, Nittrouer, Mohrig, & Shaw, 2012; Martin, Fernandes, Pickering, Howes, Mann, & McNeil, 2018; Nittrouer et al., 2012; Trower, Ganti, Fischer, & Lamb, 2018). During low discharge, deposition takes place in the river channel, whereas high discharge leads to drawdown of the water surface to sea level (Figure 1b), inducing flow acceleration and bed scouring (Chatanantavet & Lamb, 2014; Chatanantavet et al., 2012; Lamb et al., 2012; Nittrouer et al., 2012). These scouring surfaces deepen basinwards and differ from the general model of distributaries, which become shallower and narrower after every bifurcation (e.g. Edmonds & Slingerland, 2007; Yalin, 1992). Flood-induced scours in backwater zones have been suggested as a mechanism that can produce large erosional surfaces (Fernandes et al., 2016; Ganti et al., 2019; Lamb et al., 2012; Trower et al., 2018). These can be up to three times deeper than bankfull channel depth and may

therefore challenge the distinction between flood-induced multi-storey channels and incised-valley fills. Because incised valleys have been interpreted to evidence relative sea-level fall (e.g. Blum et al., 2013; Catuneanu, 2006; Posamentier, Jervy, & Vail, 1988; Van Wagoner et al., 1988), the adequate interpretation of these deep scours may influence the understanding of a depositional system. To distinguish flood-induced multi-storey channels and incised-valley fills, the updip extent of valley incision compared to backwater lengths is regarded a criterion (Ganti, Chu, Lamb, Nittrouer, & Parker, 2014; Ganti et al., 2019; Trower et al., 2018). This upstream limit of valley incision (knickpoint) will migrate updip over time when regression exposes a slope steeper than the contemporary river equilibrium profile and incised valleys form (Posamentier & Vail, 1988; Wescott, 1993).

The Mesa Rica Sandstone (Dakota Group, USA) encompasses an exhumed low-accommodation fluvio-deltaic system along its ~400 km depositional-dip oriented profile. Several parts of the transect have been studied in key localities (Holbrook, 1996, 2001; Holbrook et al., 2006; Van Yperen, Holbrook, Poyatos-Moré, & Midtkandal, 2019; Van Yperen, Poyatos-Moré, Holbrook, & Midtkandal, 2020) but a regional-scale synthesis has not been presented before. Complemented with newly collected data, the depositional-dip oriented profile serves as a useful testing ground to

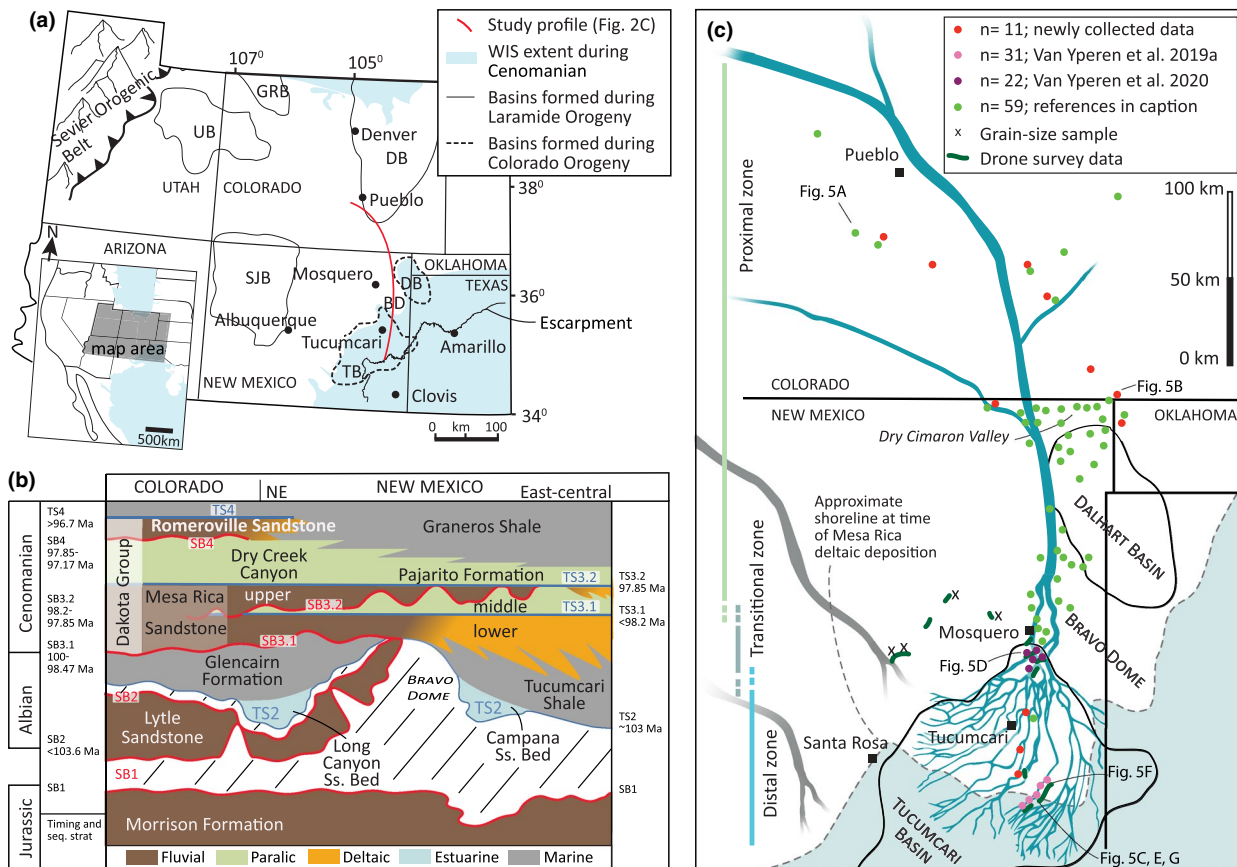


FIGURE 2 (a) Regional paleogeography showing the approximate location of the Western Interior Seaway (light blue, from Blakey, 2014) and main basins formed during Laramide and Colorado orogenies (modified after Van Yperen, Holbrook, et al., 2019). The red line indicates the studied depositional profile. BD, Bravo Dome; DB (Colorado), Denver Basin; DB (New Mexico), Dalhart Basin; GRB, Green River Basin; SJB, San Juan Basin, TB, Tucumcari Basin; UB, Uinta Basin; WIS, Western Interior Seaway. (b) Chronostratigraphy of the Jurassic to Cenomanian successions in Northeastern and East-central New Mexico. References used for compilation; Holbrook et al. (2006); Oboh-Ikuenobe et al. (2008); Waage (1955); Van Yperen, Holbrook, et al. (2019); Van Yperen, Line, et al. (2019). Albian-Cenomanian boundary from Scott et al. (2018). SB, Sequence boundary, TS, Transgressive Surface. (c) Map of study area with locations of previous and newly collected data. N indicates the total number of logs per dataset which differs from the number of logs displayed, as scale does not allow for all details. The green datasets includes logs published in Oboh-Ikuenobe et al. (2008) and Scott et al. (2004) and measured sections and 'locations where facies were identified and described but not measured' in Holbrook and Wright Dunbar (1992), Holbrook (1996, 2001) and Holbrook et al. (2006). Main structural elements are indicated (from Broadhead, 2004; Suleiman & Keller, 1985). Schematic representation of the river pathway is based on previous work (e.g. Holbrook, 1996, 2001; Van Yperen, Holbrook, et al., 2019) and reflects the extent of the depositional system (lower Mesa Rica) during regressive phase. The indicated zones (proximal, transitional, distal) are based on the study profile and explained in the text

incorporate recent insights on hydrodynamic behaviours of the fluvial realm with the establishment of a sequence stratigraphic framework for time-equivalent fluvio-deltaic strata deposited in a low-accommodation setting. Specific research objectives of this study are: (a) to describe and discuss down-dip changes in facies and depositional architecture and discuss their relationship with backwater effects and changes in base-level, (b) to establish a regional-scale (~400 km) sequence stratigraphic framework and discuss the challenges of correlating continental to shallow marine strata in a low-accommodation setting, and (c) to discuss wider implications of the diachronous character of interpreted sequence boundaries.

2 | GEOLOGICAL SETTING AND PREVIOUS STRATIGRAPHIC FRAMEWORK

The Dakota Group is one of the eastward-prograding sedimentary systems of the US Western Interior basin that were sourced from the Sevier fold-and-thrust belt (e.g. MacKenzie & Poole, 1962; Pecha et al., 2018). The fold-and-thrust belt formed during the Cordilleran orogeny, with subduction of the Farallon plate beneath west North America, causing back-arc compression in the Late Jurassic (DeCelles, 2004). The Dakota Group also received minor sediment volumes

from the Bravo Dome and Siera Grande Uplift (Holbrook & Wright Dunbar, 1992; Kisucky, 1987). The Tukumcari Basin forms the depocentre for marine strata of the fluvio-deltaic Mesa Rica Sandstone (hereafter referred to as 'Mesa Rica'; Figure 2a), the oldest formation within the Dakota Group in Colorado and New Mexico (e.g. Holbrook & Wright Dunbar, 1992). The Tukumcari Basin formed during the late Carboniferous and early Permian as a tectonic element of the Ancestral Rocky Mountains (Broadhead, 2004). At times of Dakota Group deposition, the study area was located at ~35°N latitude, with a prevailing warm and humid climate (Chumakov et al., 1995).

An overall NNW- to SSE-oriented depositional profile characterizes the Cenomanian Dakota Group (Scott, Oboh-Ikuenobe, Benson, Holbrook, & Alnahwi, 2018) in southeast Colorado and northeast New Mexico. The group is underlain by the Albian marine Glencairn Formation in Colorado and equivalent Tukumcari Shale in northeast New Mexico, and overlain by the Cenomanian Graneros Shale (e.g. Holbrook et al., 2006). The Dakota Group is further subdivided into the Mesa Rica, Pajarito (Dry Creek Canyon member in south-central Colorado and northeastern New Mexico) and Romeroville formations (Figure 2b). These represent phases of predominantly fluvial and paralic deposition. Regional sequence boundary SB3.1 (Figure 2b) forms the base of the Mesa Rica and is linked to a late Albian–early Cenomanian forced-regression, which caused widespread erosion in south-east Colorado and northeast New Mexico (Holbrook, 1996, 2001; Holbrook & Wright Dunbar, 1992; Oboh-Ikuenobe et al., 2008; Scott et al., 2004). In east-central New Mexico, the Mesa Rica is subdivided into lower, middle and upper units (Scott et al., 2004; Van Yperen, Line, Holbrook, Poyatos-Moré, & Midtkandal, 2019). The lower Mesa Rica shows a down-dip transition from fluvial to deltaic deposits at the northwestern rim of the Tukumcari Basin, recording the most proximal shallow-marine deposits within the system (Holbrook & Wright Dunbar, 1992; Van Yperen, Line, et al., 2019; Van Yperen et al., 2020). Regional sequence boundary SB3.2 forms the base of the upper Mesa Rica and is linked to another forced regression after a transgressive event that caused deposition of the paralic middle Mesa Rica (Oboh-Ikuenobe et al., 2008). These two transgressive-regressive cycles are interpreted to record higher frequency relative sea-level fluctuations than the whole Mesa Rica composite cycle (e.g. Holbrook, 1996; Holbrook & Wright Dunbar, 1992; Oboh-Ikuenobe et al., 2008; Scott et al., 2004). The SB3.2 is indistinguishable in southern Colorado where the lower and upper Mesa Rica merge into a single sandstone unit (Figure 2b; Holbrook, 2001). The down-dip extent of the SB3.1 and SB3.2 has received minimal attention to date, with the SB3.1 expression not directly mapped but interpreted as a correlative conformity at the base of the deltaic Mesa Rica (Holbrook & Wright Dunbar, 1992).

3 | METHODS

In this work we integrate previously published log data ($n = 112$), correlation panels, and interpreted photo-panoramas (Holbrook, 1996, 2001; Holbrook et al., 2006; Holbrook & Wright Dunbar, 1992; Oboh-Ikuenobe et al., 2008; Scott et al., 2004; Van Yperen, Holbrook, et al., 2019; Van Yperen, Line, et al., 2019; Van Yperen et al., 2020) with 11 newly measured stratigraphic sections. We summarize different sedimentary facies types, their associations, the occurrence of architectural elements and the extension of key stratigraphic surfaces. Together, these form the basis of a large, regional-scale (~400 km) and depositional-dip parallel correlation panel, which covers the Mesa Rica transect along its NNW-SSE oriented profile from southeast Colorado to central-east New Mexico (Figure 2c). The panel is used as the main tool to describe and discuss down-dip changes in facies distribution, depositional architecture and the sequence stratigraphic interpretation. We selected representative trunk channel (i.e. not tributary, nor distributary) elements for grain-size sampling (see 'Backwater length and its components') based on newly collected UAV (unmanned aerial vehicle, shot with a Phantom 4 Pro®) imagery at four locations. The UAV imagery allowed assessment of channel dimensions and hierarchy.

3.1 | Backwater length and its components

The backwater length (L_b) scales approximately with $L_b = h_{bf}/S$, where h_{bf} is bankfull flow depth and S the river bed slope (Paola & Mohrig, 1996). S and h_{bf} are evaluated upstream in a reach of normal flow (e.g. Trower et al., 2018). L_b is the approximate part of the river comprised between the river mouth and the point where mean sea level intersects the riverbed profile. To calculate the slope, we use an empirical equation (Holbrook & Wanas, 2014; Trampush, Huzurbazar, & McElroy, 2014):

$$\tau_{bf50}^* = (h_m S) / (PD_{50}) \quad (1)$$

where S is slope, P is submerged dimensionless density of sand-gravel sediment, and h_m is the average bankfull channel depth of the trunk river. D_{50} is average grainsize for the lowermost portion of a channel, which represents the coarsest material transported as bedload. Note that the average bankfull channel depth is one-half of the maximum bankfull thalweg depth (Bridge & Tye, 2000; Holbrook & Wanas, 2014; Leclair & Bridge, 2001) and not the average of multiple maximal bankfull measurements (cf Lin & Bhattacharya, 2017). The Shields number for dimensionless shear stress (τ_{bf50}^*) is 1.86 (Holbrook & Wanas, 2014 and references herein). Sediment density is assumed to be 2.65 g/cm³, given that the sediment is quartzose

(e.g. MacKenzie & Poole, 1962; Van Yperen, Line, et al., 2019). This gives a submerged density (P) of 1.65 g/cm^3 that is entered into Equation (1) as dimensionless number of 1.65. D_{50} grain-size values are derived for four samples (Figure 2c), taken from approximately 10–15 cm above the basal scour surface of selected trunk channel-fill sandstone bodies in the lower Mesa Rica.

Bankfull channel depth was measured directly at completely preserved trunk channel deposits from outcrop and from ortho-rectified drone imagery. Where stories recorded incomplete preservation due to episodes of cut and fill, cross-set thicknesses were measured. We used these to calculate mean dune height (Leclair & Bridge, 2001) and subsequent bankfull paleoflow depths (Allen, 1982; Best & Fielding, 2019; Bradley & Venditti, 2017). By using these bankfull paleoflow depths with respect to valley scour depths, allogenic or autogenic backwater effects as the forcing mechanism for large erosional surfaces can be discussed (Fernandes et al., 2016; Ganti et al., 2019; Lamb et al., 2012; Trower et al., 2018).

4 | FACIES ASSOCIATIONS

The description and interpretation of facies and their associations are summarized from the newly collected sedimentary logs and integrated with previous studies (Holbrook, 1996, 2001; Holbrook et al., 2006; Holbrook & Wright Dunbar, 1992; Oboh-Ikuenobe et al., 2008; Scott et al., 2004; Van Yperen, Holbrook, et al., 2019; Van Yperen et al., 2020). They are presented in Table 1. We distinguish seven facies associations: prodelta (FA1), delta front – river dominated (FA2), delta front – river dominated, wave-reworked (FA3), fluvial channels (FA4), marine-influenced distributary channels (FA5), lower delta plain and interdistributary bay (FA6), estuarine deposits (FA7), beach (FA8) and lagoon (FA9). Facies associations (FA1–9) reflect environments of deposition, based on the combination of dominant sedimentary processes (facies), bioturbation intensity, and lateral and vertical facies relationships (Table 1; Figures 3 and 4).

5 | FLUVIAL CHANNEL STYLE

Previous publications provided extensive descriptions about fluvial architectural style at different locations within the study area (Holbrook, 2001; Van Yperen, Holbrook, et al., 2019; Van Yperen et al., 2020). Based on sandstone-body dimensions and vertical and lateral spatial arrangements, we distinguish six different types of channel deposits (Figure 5): multivalley sheet (channel type I), single-story sheet of trunk channels (channel type II), isolated fluvial distributary channels and channel belts (channel type III), incised valley

(channel type IV), fluvial distributary-channel sheet (channel type V), and marine-influenced distributary channels and channel belts (channel type VI). Figure 5 provides a summary of their main characteristics. Incised-valley deposits are distinguished from channel deposits based on their multistory and multi-lateral infill (Fielding, 2008; Holbrook, 2001) and their estimated channel tops below the surrounding topographic surface (Martin, Cantelli, Paola, Blum, & Wolinsky, 2011; Strong & Paola, 2008; Van Yperen, Holbrook, et al., 2019).

6 | STRATIGRAPHIC ARCHITECTURE

The study interval is represented by a tabular and laterally extensive package of strata across the ~400 km depositional-dip profile (Figures 6a,b and 7a–e). The studied transect is divided broadly into three geographical zones, proximal, transitional, and distal, based on the dominant facies associations and depositional style that distinguish them (Figure 6a,b). The characteristics of the defined zones are described below and interpreted in terms of changes in depositional mechanisms and/ or available accommodation. As this study only focuses on the Mesa Rica deposits, the stratigraphic relationships with underlying and overlying strata are only locally incorporated to provide stratigraphic context, and not described in detail.

6.1 | Proximal zone

6.1.1 | Description

The proximal zone is defined by exclusively fluvial channel-fill deposits (FA4) in the lower and upper Mesa Rica (Figure 6a,b; Table 1). In the updip reaches of this zone, 11–22 m-thick multivalley-sheet deposits (channel type I; Figure 5a) are present. In the downdip reaches of the proximal zone, single-story sheet of trunk channels (channel type II; Figure 5b) of the lower Mesa Rica form a >80 km wide, laterally continuous 10–15-m-thick sheet that thins to 6–10-m-thick towards the transitional zone (Figure 6a,b; Holbrook, 1996; Van Yperen et al., 2020). The continuous sandstone sheet is one story thick and channel-fill elements locally aggrade into the overlying fine-grained facies (Holbrook, 1996). Trunk-channel fill deposits have an average aspect ratio (width-to-thickness) of 16.7. Fine-grained paralic strata (FA6) separate the lower from the upper Mesa Rica (Figure 6b). The latter forms one-story-thick localized channel belts (channel type II, Figure 5a) with a total thickness 4–7 m. In the lower Mesa Rica, interfluvial facies such as overbank fines, splay deposits and/or abandoned channel-fill facies are rare. Cross-bedding orientations (FA4) indicate unidirectional palaeocurrents with a mean SSE-orientation (Figure 6b).

TABLE 1 Summary of facies associations for the Campana Sandstone Bed, Tucumcari Shale, Mesa Rica Sandstone and Pajarito Formation. Note the reference to figures with photographs of each facies association

Facies association	Structures/description	Thickness and geometries	Boundaries and distribution	Biogenic structures	Interpretation	Figure
FA1 Prodelta/ offshore	Transitional zone: gray, structureless muddy siltstone. Distal zone: dark gray to black fissile mudstone with varying silt content. Locally interbedded with bioturbated sandstone beds with bivalve fragments.	Packages are 0.3–1.8 m thick (transitional zone), to 20 m thick (distal zone). Individual sandstone beds 10–20 cm.	In sharp contact with FA2 (transitional zone), vertically and laterally gradational into FA2, FA3 (distal zone). Pinches out northwest of transitional zone.	Transitional zone: BI 4–5; <i>Thalassinoides</i> , <i>Phycosiphon</i> , <i>Planolites</i> , <i>Teichichnus</i> , <i>Chondrites</i> , <i>Helminthopsis</i> Distal zone: <i>Texigryphaea</i> , <i>Pelinitia levicostata</i> , <i>Protocardia texana</i> , <i>Ostrea Marshii</i> Sandstone beds BI 4–6 undifferentiated.	Deposition in a prodeltaic setting, below fair-weather wave-base (distal zone). Shallow setting in the transitional zone, based on thin and silty appearance, lack of macrofauna indicative of open marine settings (e.g. Holbrook et al., 1987). The bioturbated sand- and shell-beds represent short-lived storm deposits (Van Yperen, Holbrook, et al., 2019).	Figure 3a,f
FA2 Delta front—river dominated	Very fine- to fine-grained sandstone beds with a sharp tabular nature. Transitional zone: structureless near the base, progressively more planar- and tangential, cross-stratified - locally with pebbles - upwards. In places interbedded with siltstone to very fine-grained sandstone, asymmetrical ripples. Sparse mud-drapes. Locally: matrix- to clast-supported conglomerate alternating with structureless sandstone beds with a sharp or gradational contact surface. Distal zone: symmetrical ripple lamination, locally mud-draped current ripples.	Packages are 6–11 m thick and sheet forming. Individual sandstone beds 5–50 cm.	Commonly abruptly succeeded vertically by FA4. Grades laterally into FA1. Dominant in transitional zone, rare in distal zone, absent in proximal zone.	Transitional zone: BI 0–5, non-uniform but upwards-decreasing trend; <i>Ophiomorpha</i> , <i>Thalassinoides</i> , <i>Conichnus</i> , <i>Palaeophycus</i> , <i>Macaronichnus</i> , <i>Teichichnus</i> , <i>Rosellia</i> . Distal zone: BI 0–1, non-uniform; <i>Ophiomorpha</i> .	Deposits of an active river-dominated delta front. Transitional zone: variation in bed thickness, occurrence of interflow beds, bioturbation index and tide-influence reflect differences in hydraulic conditions at mouth bar scale (Van Yperen et al., DepRecord). Increasing river proximity inferred from upwards-decreasing BI and upwards-increasing pebble content. No indicators for wave-influence. Distal zone: minor wave influence and minor tide-influence.	Figure 3b–e,g

(Continues)

TABLE 1 (Continued)

Facies association	Structures/description	Thickness and geometries	Boundaries and distribution	Biogenic structures	Interpretation	Figure
FA3 Delta front—river-dominated, wave-reworked	Coarsens upward from very fine sandstone with a silt component to a clean fine-grained sandstone. Intense bioturbation obliterates original bedding structures. Repetitive 5–15-cm-thick normally graded sandstone beds, mainly in lower part. Local 10–60-cm-thick shellbeds.	Packages are 6–14 m thick. Sheet forming, configuration into tabular geometries.	Incised by FA4 in most places. Absent in proximal and transitional zones.	BI 2–6, upwards decreasing; <i>Ophiomorpha</i> , <i>Thalassinoides</i> , <i>Cylindrichnus</i> , <i>Pelaeophycus</i> , <i>Skolithos</i> , <i>Rhizocorallium</i> . Local shell beds: <i>Scabrotrigonia-Turritella</i> middle-shoreface faunal association (Scott, 1974).	Distal to proximal delta front deposition, above fair-weather wave-base. High BI suggest wave-agitation, as this optimizes infauna living conditions (e.g. MacEachern & Bann, 2008). Sheet-like nature resulted from successive coalescence of mouth bars (Olariu & Bhattacharya, 2006). Lateral sand redistribution by waves caused configuration into tabular geometries.	Figures 3h and 7c–e,g,h
FA4 Fluvial channels	Fine- to medium-grained sandstone beds with parallel lamination, tabular and trough cross-stratification, organized in sandstone bodies bound by erosional flat- and concave-upward surfaces. Upper beds within these are parallel or ripple-laminated sandstone. No mudstone drapes or heterolithic bedding.	Lensoid 1–22 m thick (composites). Individual sandstone beds 10–100 cm thick. Multi-lateral, single-story, multi-story, isolated	Incises into delta front (FA2, FA3) or lower delta plain deposits (FA6). Present throughout study area.	Locally roots, rhizocretions and/or <i>Skolithos</i> (BI 0–2) at top surface. Varicoloured mottling overprints uppermost interval of FA4 units in places.	Deposition from migrating 2D and/or 3D subaqueous bedforms (dune and ripple-scale) and formation of parallel laminations in upper flow regime conditions, within subaqueous channels (e.g. Flemming, 2000). Absence of bioturbation and mud-drapes suggests deposition by fully fluvial currents. Weak pedogenesis indicates subaerial exposure. Trace fossils relate to later flooding.	Figures 4a–c and 5a–f
FA5 Marine-influenced distributary channels	Very fine- to fine-grained sharp-based, structureless or cross-stratified sandstone beds that alternate with flaser bedding and/or thin siltstone intervals. Occasional (double) mud-drapes, unidirectional and/or bidirectional ripples. Wood debris, syneresis cracks, mud rip-up clasts. Distal zone: no flaser bedding, no bidirectional ripples, siltstone ripples are rare.	Lensoid 1–12 m thick (composites). Individual sandstone beds 10–40 cm thick, siltstone intervals 1–10 cm thick. Single-story, multi-story (2–3), multilateral isolated	Predominantly incised into muddy siltstones (FA6) and rarely into delta front deposits (FA2). Sparse occurrence through study area, absent in upper reaches of proximal zone.	Transitional zone: BI 0–3, non-uniform; <i>Skolithos</i> , <i>Macaronichnus</i> , <i>Ophiomorpha</i> . <i>Teredolites</i> -bored wood fragments. Distal zone: BI within lower beds of FA5 units.	Marine-influenced distributary channel-deposits with varying tidal modulation. Stronger tide-influence in the transitional-zone channel bodies than in the distal zone. Brackish-water conditions allowed only limited bioturbation and low-diversity ichnofauna (MacEachern, Bann, Bhattacharya, & Howell, 2005).	Figures 4f and 5g

(Continues)

TABLE 1 (Continued)

Facies association	Structures/description	Thickness and geometries	Boundaries and distribution	Biogenic structures	Interpretation	Figure
FA6 Lower delta plain and inter-distributary bay	Predominantly gray-brown muddy siltstone. Locally, very fine- to fine-grained, sharp-based sandstone beds with bed tops with asymmetrical ripples. These beds are structureless, rarely cross-stratified, and interbedded with rippled siltstone. Distal zone. coarsening-upward successions grade from silty mudstone into interbedded very fine-grained sandstone beds with silty mudstone layers.	Sandstone beds; 5–15 cm thick, 100–200 m lateral extent. Coarsening-upward packages; <1.5 m, laterally up to few tens of meters.	Transitional and distal zone. Eroded by FA4 and FA5.	BI 0–3, <i>skolithos</i> , <i>Arenicolites</i> , <i>Phycodes</i>	Lower-delta-plain to interdistributary-bay deposits with crevasse splays and overbank flow deposits. Localized shallowing-upward events may represent bayhead deltas and distal bay infill (e.g. Aschoff, Olariu, & Steel, 2018).	Figure 4c
FA7 Estuary	Fine-grained sandstone, primary sedimentary structures obliterated by bioturbation. In places fining-upwards to very-fine grained sandstone beds (5–20 cm). If not bioturbated, sandstone beds are parallel-laminated, planar- and tangential cross-stratified.	Packages are 2–7 m thick. Lensoid and tabular	Local occurrence in transitional zone. Onlaps and incises into underlying Jurassic strata, overlain by FA1.	BI 0–1 or BI 5–1; <i>Thalassionoides</i> , <i>Ophiomorpha</i>	Estuarine deposits, based on localized occurrence, upward-increasing marine influence, and stratigraphic position below prodelta deposits (FA1) (e.g. Holbrook et al., 1987)	—
FA8 Beach	White to light-gray parallel-laminated, low-angle or tangential cross-stratified sandstone, dipping both paleolandward and seaward.	1.5–3 m thick packages, up to 2 km along depositional dip. Tabular	Locally present in distal zone, progressively fragmented and eventually absent in depositional dip direction.	Roots or <i>Skolithos</i> (BI 0–3), locally weak pedogenesis.	Foreshore and backshore deposition, with occasional wash-over fans, rooted eolian dunes and short-lived marine incursions.	—
FA9 Lagoon	Fining-upward interbedded sandstone and siltstone. Occasional bidirectional ripples. More sand-prone towards distal end study profile.	~5-m-thick packages	Distal reaches of the distal zone. Absent in proximal and transitional zones.	Flaser and wavy bedding: BI 0–2; <i>Skolithos</i> , <i>Ophiomorpha</i> Lenticular interval: BI 1–4; <i>Phycosiphoni</i> , <i>Thalassinoides</i> , <i>Teichichnus</i> , <i>Siphonichnus</i> .	Vertical transition from flaser, through wavy, to lenticular bedding. Deposition in a sheltered, tide-influenced environment.	Figure 4d

6.1.2 | Interpretation

The multivalley-sheet deposits (channel type I) represent buffer valleys (*sensu* Holbrook et al., 2006) and amalgamation of the lower and upper Mesa Rica into one sandstone unit (Holbrook, 2001). Temporal fluctuations in upstream

sediment and water discharge control incision and aggradation and hence the internal architecture of the buffer valleys (Holbrook, 2001). They form outside the influence of downstream controls (Figure 5). The laterally continuous sheet of single-story trunk channel deposits (channel type II) reflects significant avulsion. We interpret this as evidence

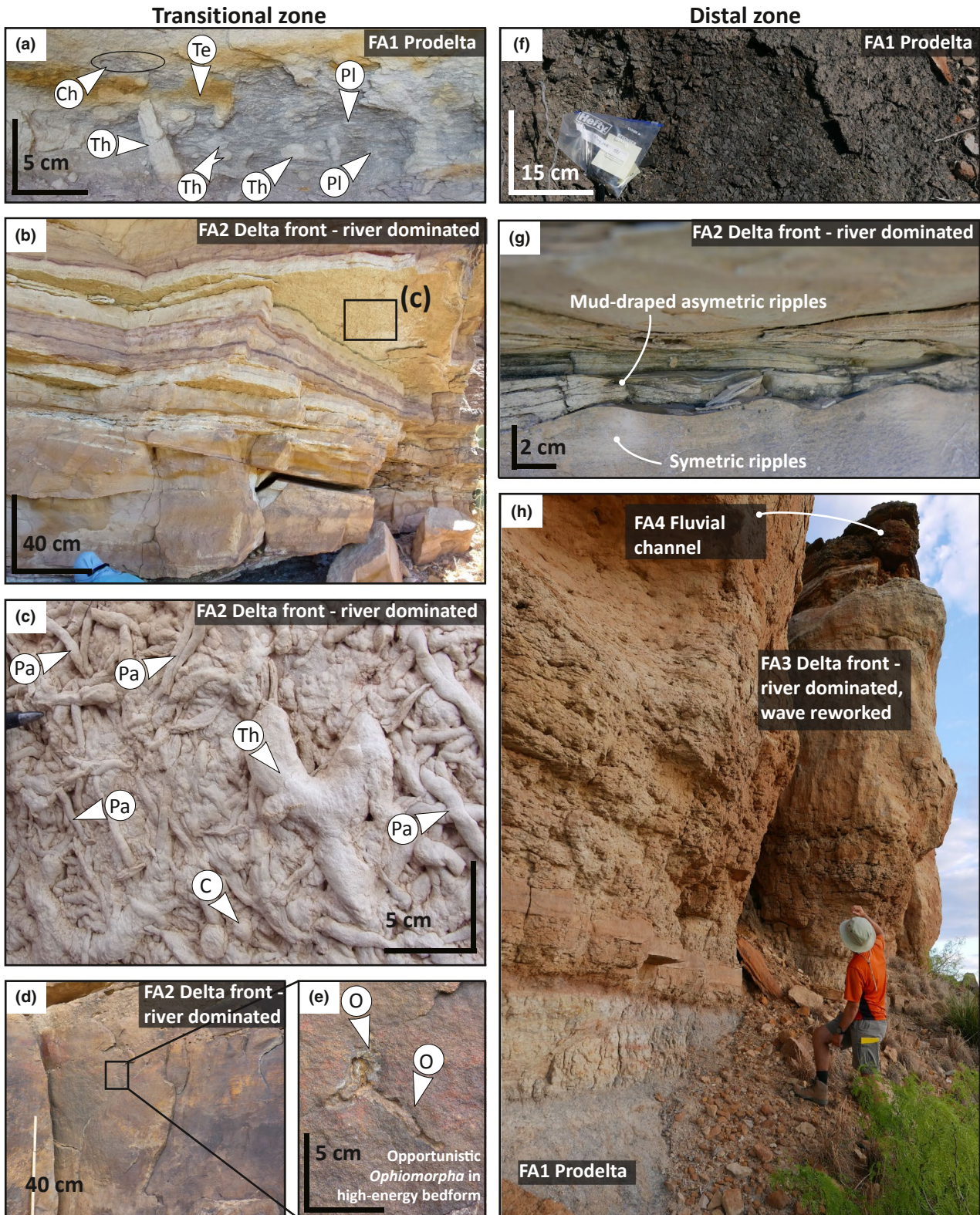


FIGURE 3 Photographs of prodelta (FA1), river-dominated delta front (FA2) and river-dominated, wave-reworked delta front (FA3) deposits in the transitional (a–e) and distal (f–h) zones. (a) Muddy bioturbated (BI 4–5) siltstone within prodelta deposits (FA1). (b) Tabular and sharp-bedded fine-grained sandstones in river-dominated delta front deposits (FA2). Bioturbation is non-uniform, but basal bedding planes are thoroughly bioturbated (BI 4–5). (c) Detail of bioturbated basal bedding planes in (b). (d) Plane-parallel laminated sandstone with sparse (BI 1) opportunistic *Ophiomorpha* in river-dominated delta front deposits (FA2). (e) Detail of traces in (d). (f) Black fissile mudstone prodelta deposits (FA1). (g) Symmetrical (wave) ripples overlain by single and double mud-draped asymmetric (current) ripples, in river-dominated delta front deposits (FA2). (h) Coarsening-upward delta front deposits consisting of prodelta mudstones (FA1) gradually transitioning to river-dominated wave-reworked delta front sandstones (FA3) abruptly overlain by fluvial distributary channels (FA4). C, *Conichnus*; Ch, *Chondrites*; He, *Helminthopsis*; O, *Ophiomorpha*; Pa, *Palaeophycus*; Pl, *Planolites*; R, *Rosselia*; S, *Skolithos*; Te, *Teichichnus*; Th, *Thalassinoides*. 15-cm pencil and 33-cm hammer for scale. (a, b) modified after Van Yperen, Line, et al. (2019), (c) modified after Van Yperen et al. (2020) (h) after Van Yperen, Holbrook, et al. (2019)

for deposition in the updip reaches of the backwater zone, because entering of the backwater zone increases avulsion and limits channel incision and/or aggradation (e.g. Chatanantavet et al., 2012; Jerolmack & Swenson, 2007). The localized channel belts (channel type III) of the upper Mesa Rica represent reoccupation of preferred channel paths and sedimentation patterns indicating higher A/S ratios than in the lower Mesa Rica.

6.2 | Transitional zone

6.2.1 | Description

The transitional zone encompasses the area over which river-dominated delta-front deposits (FA2) replace fluvial deposits (FA4) of the lower Mesa Rica (Figure 6b; Table 1). These delta-front facies form a sandstone-prone, sharp-based 6–10-m-thick deltaic package (Figure 7a,b; Van Yperen, Line, et al., 2019; Van Yperen et al., 2020). The sandstone beds are tabular and laterally extensive. Upper flow regime bedforms dominate and interbedding with finer-grained facies is rare (Figure 3b–e). The underlying prodelta deposits (FA1; Figures 3a and 6b) belong to the Tucumcari Shale and pinch out to the northwest which coincides with the Tucumcari Basin rim. Localized estuarine deposits (FA7) occur below the Tucumcari Shale (Figures 6b and 7a,b). Composite erosional surfaces form valleys that incise locally into underlying strata and are infilled with multi-storey fluvial (FA4) and marine-influenced channel deposits (FA5; Figures 5d,e and 6b). The composite scours of these incised-valley deposits (channel type IV) are 12–20 m thick, 100–300 m wide. Rare single-story trunk channel deposits (channel type II) occur isolated and incised into underlying delta deposits (Figure 6b).

The upper Mesa Rica consists of discontinuous fully fluvial channel-belt deposits (FA4, channel type III; Figure 7a,b) and tide-influenced channel-fill deposits (FA5, channel type VI; Figure 4f) embedded within interdistributary fines (FA6; Figure 6b). Channel belt deposits (channel type III) have average axial thickness of 4 m and true cross-stream widths

of 100 m, which gives an average aspect ratio of 25. Tide-influenced channel-fill deposits (channel type VI) have an average aspect ratio of 25 as well, with average axial thickness of 2 m and true cross-stream widths of 50 m, respectively.

6.2.2 | Interpretation

The transitional zone represents the fluvial-marine transition zone of the Mesa Rica depositional system. The delta-front deposits represent deposition close to the river outlet, based on the dominance and near-absence of upper flow regime bedforms and fine-grained facies, respectively (Van Yperen et al., 2020). The resemblance of prodelta deposits pinch out and the location of the Tucumcari Basin rim indicates a close relationship between basin configuration and open-marine sediment deposition (e.g. Holbrook & White, 1998; Holbrook & Wright Dunbar, 1992; Kisucky, 1987). The underlying estuarine deposits represent transgressive infill of topographic lows (Holbrook, Wright, & Kietzke, 1987; Van Yperen, Line, et al., 2019). In the incised valleys (channel type IV), erosion and deposition occurred at depths below the topographic surface of the valleys (see ‘incised valleys; paleoflow depth and knickpoint migration’ for further details). The dispersed trunk channel deposits (channel type II) represent continued progradation and feed a more distal part of the delta. The upper Mesa Rica represents an upper to lower delta plain depositional environment.

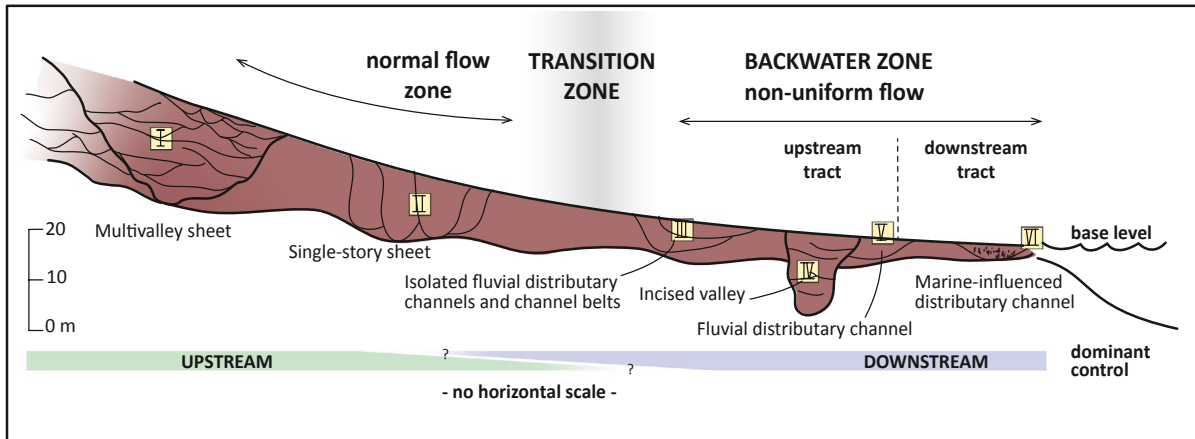
6.3 | Distal zone

6.3.1 | Description

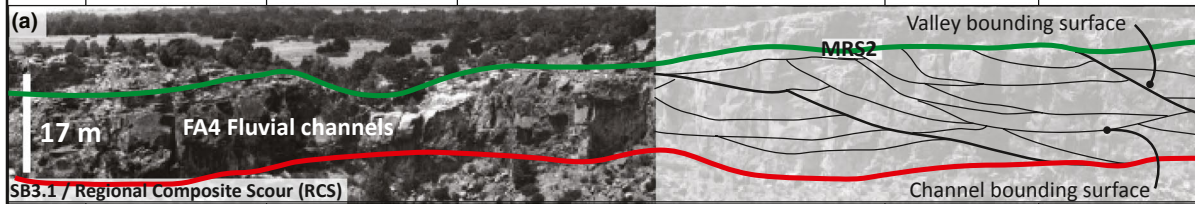
The distal zone is where the lower Mesa Rica represents its fully deltaic development (Van Yperen, Holbrook, et al., 2019) (Figure 6b). Here, prodelta mudstones (FA1; Figure 3f; Table 1) are up to 21 m thick, with a discontinuous pebble lag at their base. These dark grey to black fissile mudstone deposits grade vertically into river-dominated, wave-reworked delta-front deposits (FA3) of the lower Mesa



FIGURE 4 Photographs of selected facies associations in the distal (a–d) and transitional (f–h) zones. (a) Stacked fluvial distributaries in erosional contact with underlying delta front sandstones (FA3) in the distal zone. (b) Rhizocretion (root concretion) in cemented top interval of a fluvial distributary channel (FA4) in the distal zone. 33-cm hammer for scale. (c) Coarsening-upward packages in erosional contact with fluvial distributary channel deposits (FA4). These are interpreted as bayhead deltas and occur in interdistributary bay deposits (FA6) in the distal zone. (d) Lenticular bedding with sporadic bioturbation (BI 1–4) in lagoonal deposits (FA9). (e) Sharp-based, structureless and internally ripple-laminated sandstone beds, with up to moderate bioturbation (BI 0–3), in lower delta plain deposits (FA6) in the transitional zone. (f) Heterolithic deposits of tide-influenced distributary channel fill (FA5), in the transitional zone. Ph, *Phycosiphon*, Si, *Siphonichnus*; Te, *Teichichnus*, Th, *Thalassinoides*. (d) modified after Van Yperen, Holbrook, et al. (2019), (f) modified after Van Yperen et al. (2020), (f) after Van Yperen, Line, et al. (2019)



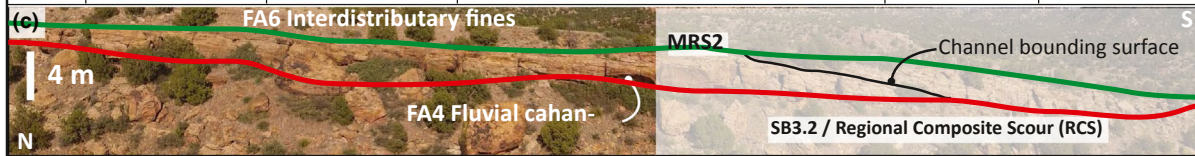
Channel type	Fluvial architecture, location in study area, figure	Stacking pattern, dimensions (W:T)	Main characteristics and sketch	Depositional mechanism	Main control
I	Multivalley sheet Proximal zone, up dip from Channel type II	Multi-storey, multi-lateral Average: > 80 km : 15 m Max: > 80 km : 22 m	 FA4 Fluvial channels - Stacked channel belts bundled into valleys - Incomplete channel fills	Repeated incision and aggradation cycles, likely tributary channels	Temporal changes in sediment and water discharge, undifferentiated climate, tectonic, and/or autogenic control



II	Single-story sheet of trunk channels Proximal zone, up dip from Channel type III	Single-story, mostly multi-lateral, rarely dispersed Average: 250 : 12 m Max: 300? : 15 m	 FA4 Fluvial channels - Channels have low aspect ratio - Similar geometries and dimensions	Successive cut-and-fill-events of single-stream trunk channels	Upstream and downstream factors, limited vertical space due to converging upper and lower buffer profiles
----	---	---	---	--	---



III	Isolated fluvial distributary channels and channel belts Transition and distal zones	Mostly single-story, max 3 stories, multi-lateral Transition zone: Average: 100 : 4 m Max: 400 : 7 m Distal zone: Average: 50 : 2,5 m Max: 150 : 7 m	 FA6 Interdistributary fines FA4 Fluvial channels - Independent channels and adjacent to lateral-accretion elements	Cut-and-fill-events within the upstream tract of the backwater zone	Reoccupation of preferred channel paths, higher A/S ratios than channel type 5
-----	---	--	--	---	--



CONTINUATION OF FIGURE 5


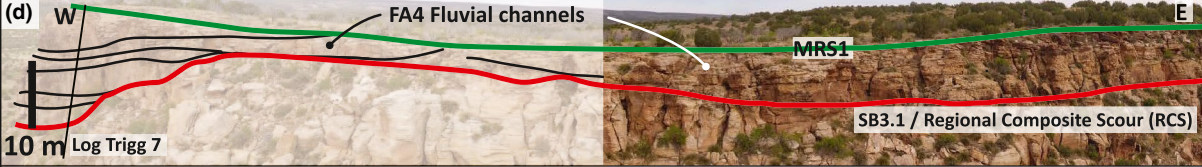
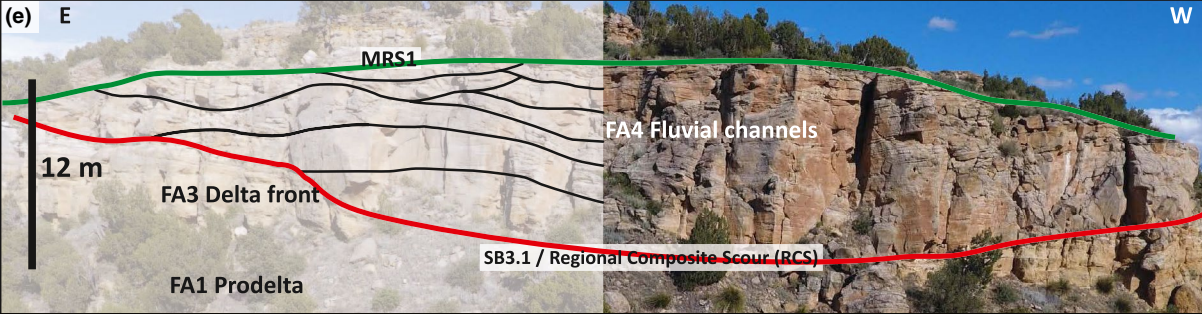


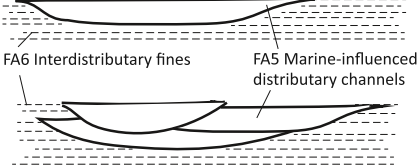

Channel type	Fluvial architecture, location in study area, figure	Stacking pattern, dimensions (W:T)	Main characteristics and sketch	Depositional mechanism	Main control
IV	Incised valley Transition and distal zones	Multi-storey, multi-lateral Transition zone: Average; 200 : 16 m Max; 300 : 20 m Distal zone: Average; 140 : 11 m Max: 250 : 12 m	 Predominantly FA4, rare FA5 - Scarce lateral-accretional elements - Isolated, scoured into deltaic sediments	Erosion and deposition at depths below the topographic surface	Sea-level drop over slopes steeper than the contemporary river equilibrium profiles
(d)					
(e)					
V	Fluvial distributary-channel sheet Distal zone	Mostly single-story, max 2 stories, multi-lateral Average: 70 : 4 m Max: 150 : 6 m	 FA4 Fluvial channels - No lateral-accretion elements - Forms continuous sheet	Lateral amalgamation of distributary channel fill deposits within the upstream tract of the backwater zone	Low depositional gradient and high sediment supply favors rapid infill of newly formed distributary channels and high-frequency avulsion patterns
(f)					
VI	Marine-influenced distributary channel Transition and distal zones	Transition zone: single-story Distal zone: 2-3 stories, multi-lateral Transition zone: Average; 50 : 2 m Max; 70 : 3 m Distal zone: Average; 30 : 2 m Max; 50 : 3 m	 FA6 Interdistributary fines FA5 Marine-influenced distributary channels - No lateral-accretion elements - Transition zone: weak to moderate tide influence - Distal zone: absent to weak tide influence	Cut-and-fill-events within the downstream tract of the backwater zone	Mixing of fresh and saline waters at times of decreased river discharge
(g)					

FIGURE 5 Overview of all distinguished channel types in this study, accompanied with a representative photograph with annotated main bounding surfaces. The slope of the longitudinal profile is schematic as there is no horizontal scale applied. W:T (width:thickness) ratios refer to the total composite dimensions for Channel type I, III, IV and VI and to individual channel elements in Chanel Type II and V. (a) Multivalley sheet (channel type I) in which the lower and upper Mesa Rica are merged and the intervening SB3.2 sequence boundary is indistinguishable. Sandstone deposits above MRS2 belong to the Romeroville Formation. Interpretation with details on higher-order internal architecture in Holbrook (2001; Figure 6). Proximal zone, Huerfano Canyon (Colorado). (b) Single-story sheet of trunk channels (channel type II) in the proximal zone, Purgatoir Canyon (Colorado). (c) Isolated channel belt (channel type III) of the upper Mesa Rica embedded within interdistributary fines (FA6) in the distal zone, Dog Canyon (New Mexico). (d) ~20-m-thick incised valley-fill (channel type IV) in the transitional zone, Trigg Ranch Horseshoe Cliff (New Mexico). The basal erosional regional composite scour (RCS) bounds a multi-storey infill composed of bar forms and channel elements (FA4) and scoured into underlying fluvial Jurassic strata. (e) ~12-m-thick incised valley-fill (channel type IV) in the distal zone, Apache Canyon (New Mexico). The regional composite scour (RCS) scoured into underlying delta front deposits (FA1, FA3). The infill consists of stacked barforms and channel elements with locally adjacent barforms in the uppermost stories. Detailed overdrawing in Van Yperen, Holbrook, et al. (2019); Figure 10). (f) Sheet-forming distributary channels (channel type V) in the distal zone, Stanley's Turbines (New Mexico). Their composite underlying scours form the Basal Distributary Composite Scour (BDCS). (g) Multi-storey, multi-lateral marine-influenced distributary channel (channel type VI) in the distal zone, Apache Canyon (New Mexico). See Figure 2c for outcrop locations. MRS, maximum regressive surface. (a) modified from Holbrook (2001), (e), (f) and (g) modified from Van Yperen, Holbrook, et al. (2019)

Rica (Figure 3h). The delta front deposits form 6–14-m-thick sheet-like sandstone unit throughout the distal zone (Figures 6b and 7c–e). The overlying sand-filled distributary-channel deposits (FA4) are laterally amalgamated, rework the upper delta-front deposits and form a continuous sheet in places (Figure 5f, channel type V). Their individual channel-fill elements have average aspect ratios of 17.5. In the distal reaches of the distal zone, downstepping delta-front strata are 2–8 m thick and overlain by lagoonal deposits (FA9; Figures 4d and 6b). Erosional composite surfaces bound the multi-storey infill of incised valleys (FA4; channel type IV), incise deeply into underlying deltaic strata, and have thicknesses between 8 and 12 m and total widths between 90 and 250 m (i.e. aspect ratios of 7.5–31; Figures 5e and 6b). Their sediment infill is sandstone-prone and predominantly fluvial, although sparse sandstone beds with *Skolithos* trace fossils (BI 1–2) occur. Drone survey imagery reveals the rare occurrence of incised-valley fill deposits (FA4; channel type IV) fining upwards to mud- or silt-dominated facies.

The upper Mesa Rica consists of a laterally varying spectrum of interdistributary bay deposits (FA6; Figure 4e), beach deposits (FA8) and laterally disconnected fully fluvial (FA4, channel type III; Figure 5c) or marine-influenced distributary channel deposits (FA5, channel type VI; Figure 6b). Isolated channel belt deposits (channel type III) have average axial thickness of 2.5 m and cross-stream width of 50 m (aspect ratio of 20; Figure 5a). Marine-influenced distributary channel deposits (channel type IV) have average axial thickness of 2 m and cross-stream widths of 30 m (aspect ratio of 15; Figure 5b). Palaeocurrent measurements (FA4) indicate an average SSW orientation (Figure 6b).

6.3.2 | Interpretation

The increased thickness of prodelta mudstones towards the SE is consistent with the deepening of the basin. The

sheet-like delta-front sandstone geometries overlain by sand-filled amalgamated distributary channel deposits (channel type V) result from enhanced mouth-bar depositional cycles and highly avulsive distributary channels. The low-accommodation setting favoured these depositional mechanisms (Olariu & Bhattacharya, 2006; Van Yperen, Holbrook, et al., 2019).

The upper Mesa Rica represents a dynamic lower-delta-plain with setting in which short-lived marine incursions locally caused weak tidal influence. The A/S ratio was higher than in the lower Mesa Rica, as the upper Mesa Rica does not form continuous sheet of amalgamated sandstone body deposits. Deflection of the main paleocurrent trend mimics the basin orientation (Van Yperen, Holbrook, et al., 2019).

7 | KEY STRATIGRAPHIC SURFACES

In the Mesa Rica depositional system, several stratal discontinuities can be distinguished based on underlying and overlying facies, and stacking patterns of adjacent strata. These key sequence stratigraphic surfaces were described and interpreted at separate key localities (Holbrook, 1996, 2001; Oboh-Ikuenobe et al., 2008; Scott et al., 2004; Van Yperen, Holbrook, et al., 2019). In this study, their proposed correlation and expansion provides improved understanding of their regional extent (Figures 6c and 7).

7.1 | Maximum regressive and flooding surfaces

7.1.1 | Description

Fine-grained facies (FA6) overlie top surfaces bounding fluvial strata in the proximal zone and deltaic successions

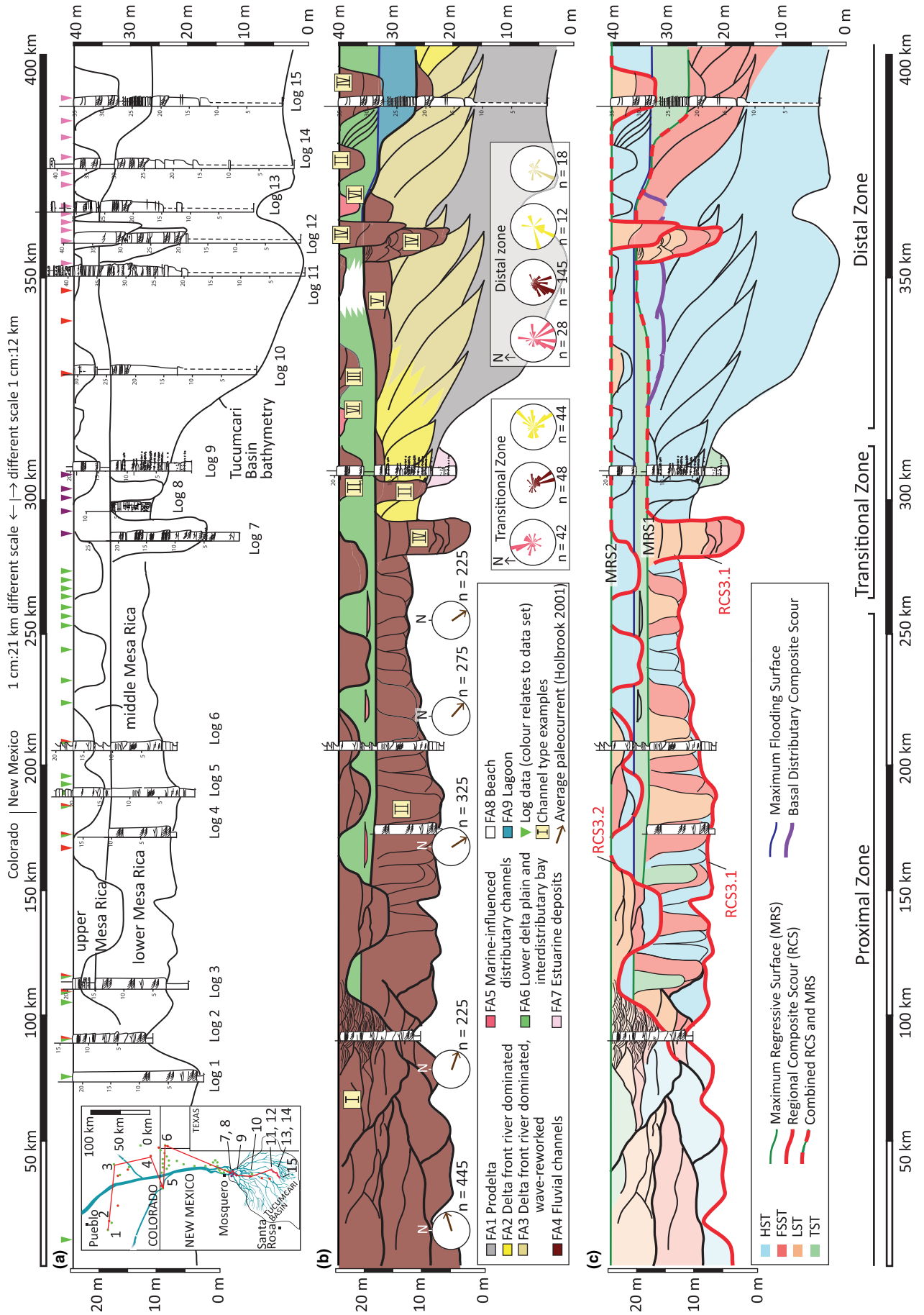


FIGURE 6 Regional-scale (~400 km), depositional dip-parallel correlation panel of the Mesa Rica fluvio-deltaic system throughout southeast Colorado to central-east New Mexico. The colour code for the logs indicates the data source, similar as in Figure 2c. Key stratigraphic surfaces and distribution of facies associations and architectural elements are based on all available log data, drone surveys and descriptions of architectural elements from both this study and previous work (Holbrook, 1996, 2001; Holbrook et al., 2006; Holbrook & Wright Dunbar, 1992; Oboh-Ikuenobe et al., 2008; Scott et al., 2004; Van Yperen, Holbrook, et al., 2019; Van Yperen, Line, et al., 2019; Van Yperen et al., 2020). Note that the presented sedimentary bodies such as channels and clinofolds are schematic and their depicted horizontal dimensions are not representative. Depicted clinofold heights take into account the erosion of the shoreline break (a) Simplified cross section with a selection of representative log data and main stratigraphic surfaces defining the lower, middle and upper Mesa Rica. (b) Lithostratigraphic cross section showing the downdip changes in facies distribution with 6 key logs. Rose diagrams display palaeocurrent data grouped according to facies associations. (c) Large-scale sequence stratigraphic interpretation for the Mesa Rica depositional system, showing the interpretation of key stratigraphic surfaces and system tracts. Note the cannibalization of the oldest fluvial-marine transition zone by younger single-story trunk channels (channel type I). Trunk channel sediment was deposited throughout the sea-level cycle (i.e. HST, FSST, LST, TST) and not only during the LST, as predicted in classic models. Deltaic and distributary channel deposits were formed during HST, FST and LST. GPS coordinates and references for log locations can be found in Appendix S1. See text for further discussion

in the distal zone, and commonly represent a sharp sandstone-mudstone contact (Figure 7a–d; e.g. Holbrook, 1996, 2001; Van Yperen, Holbrook, et al., 2019). These surfaces are locally rooted (Figure 4b), show evidence of oxidation and/or display moderate to high bioturbation (BI 2–6). In the distal zone, deposits overlying this surface consist of ~50-cm-thick finer-grained sandstone interbedded with mudstone, overlain by ~50 cm of dark grey mudstone (Figure 7f). Lagoon deposits (FA9; up to 4-m-thick) overlie this surface in the most distal outcrops (Figures 4d and 6b).

7.1.2 | Interpretation

Top surfaces bounding fluvial and deltaic strata are overlain by more distal facies. These surfaces correspond to the end of a regressive phase and are therefore interpreted as maximum regressive surfaces (sensu Catuneanu, 2006; MRS1, MRS2; Figure 7a–f). Roots and oxidation suggest subaerial exposure. MRS1 marks the top of the lower Mesa Rica, and is traceable for ~300 km throughout the study area, but cannibalized by overlying fluvial sandstone in the upper reaches of the proximal zone (Figures 5a and 6c). MRS2 marks the top of the upper Mesa Rica, and is traceable throughout (>400 km). These stratigraphic surfaces are essentially equivalent to previously published transgressive surfaces TS3.1 and TS3.2 (e.g. Oboh-Ikuenobe et al., 2008; Scott et al., 2004), and are used as correlation data (Figure 6). Locally, some channel fills grade vertically into the overlying finer-grained facies, which complicates an interpretation of whether their top surface was formed during lowstand normal regression or subsequent transgression. Consequently, the maximum regressive surface is potentially diachronous in some places. In the most downdip exposures, MRS1 underlies the lagoonal deposits (Figure 6b), as these are interpreted to represent transgression with respect to their underlying distributary-channel deposits (Figure 6c). Where transgressive deposits are not preserved,

MRS and MFS coincide. Regional traceability of the MRSs suggests allogenic forcing (Beerbower, 1964; Holbrook & Miall, 2020; Paola, Ganti, Mohrig, Runkel, & Straub, 2018). However, the lagoon deposits at sub-regional scale can be also ascribed to localized transgressive conditions due to lateral switching of active delta progradation locations in the distal zone (e.g. Bhattacharya, 2010; Van Yperen, Holbrook, et al., 2019).

7.2 | Regional composite scours and sequence boundaries

Earlier work on the Mesa Rica system recognized and labelled two sequence boundaries (SB3.1 and SB3.2) in the proximal zones of the study area (e.g. Scott et al., 2004). In this paper, we will use the term *Regional Composite Scour* (RCS; sensu Holbrook & Bhattacharya, 2012), because of the increasing evidence for the diachronous/composite nature of sequence boundaries (e.g. Bhattacharya, 2011; Holbrook & Bhattacharya, 2012; Strong & Paola, 2008). Thus, we change the previously used SB3.1 and SB3.2 into RCS3.1 and RCS3.2, to acknowledge the time-transgressive character of these surfaces. By definition, the RCS excludes the interfluvial component of sequence boundaries (Holbrook & Bhattacharya, 2012).

7.2.1 | Description

An erosional composite scour forms the basal surface of the multivalley sheet (channel type I) and the single-story sheet of trunk channel strata (channel type II) in the proximal zone (Figures 5a,b and 6b,c; Holbrook, 1996, 2001). Additionally, erosional composite surfaces bound the multi-storey infill of incised valleys (channel type IV) in the transition and distal zone (Figures 5d,e and 6b,c), where they separate fully fluvial deposits (FA4) from underlying deltaic facies associations

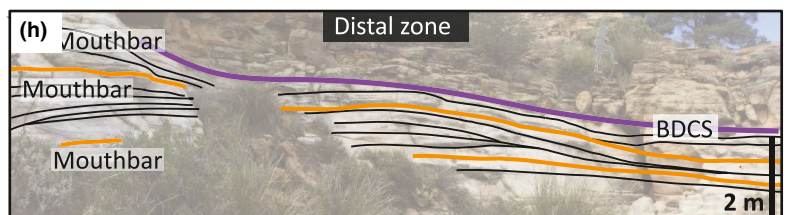
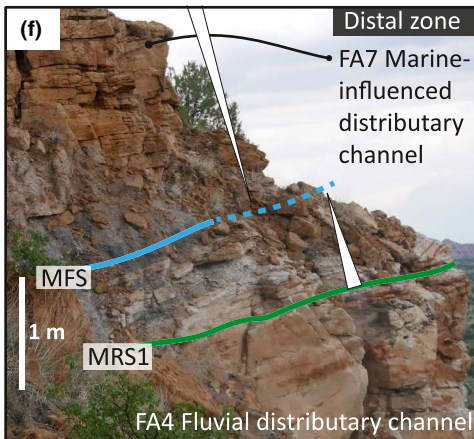
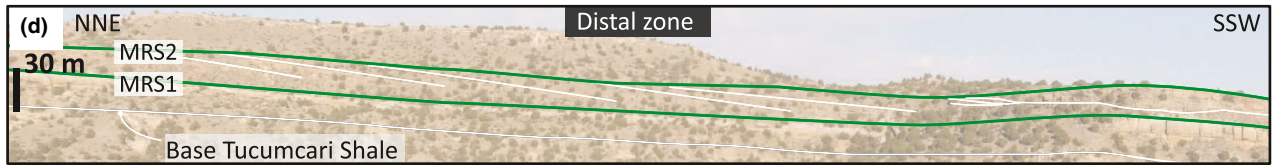
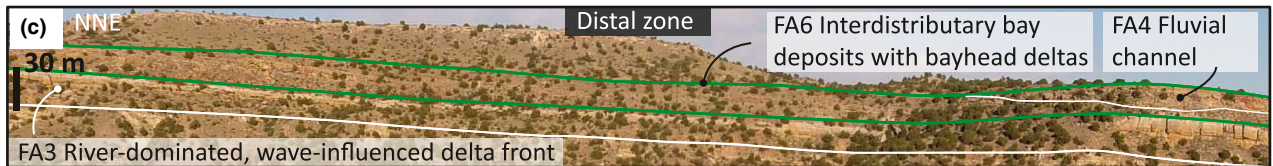
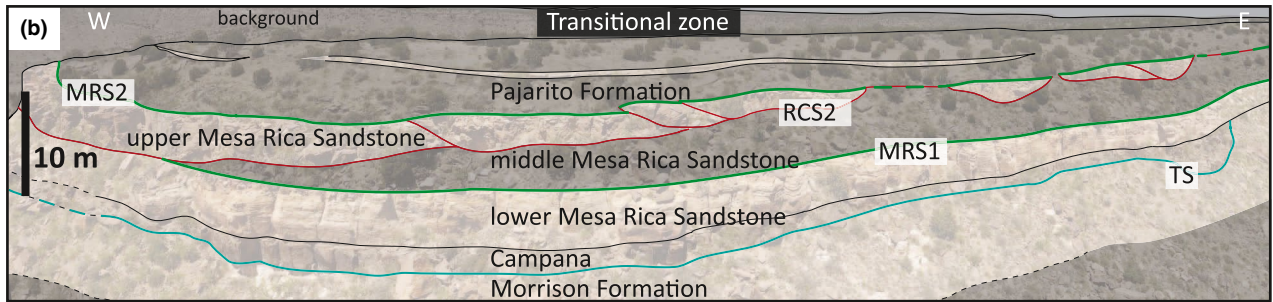


FIGURE 7 Overview of stratigraphic architecture and key stratigraphic surfaces in the transitional and distal zones. For the proximal zone, see Figure 5a,b. (a) Photograph showing the Cretaceous stratigraphy in the transitional zone. (b) Interpretation of (a). Note that the RCS excludes interfluvial. The contact between the estuarine (FA7) Campanian and deltaic (FA2) lower Mesa Rica represents a turnaround from transgressive to regressive conditions. Note the limited thickness of the delta front deposits (FA2) compared to the deltaic succession of the lower Mesa Rica in the distal zone (Figure 7c,g,h). (c) Photograph showing differences in A/S ratio between the first progradational succession (lower Mesa Rica) consisting of amalgamated sheet-forming delta-front sands (FA3) and the following progradational succession (upper Mesa Rica). The latter consists of interdistributary bay deposits (FA6) with basinward-dipping heterolithic clinoliths interpreted as small bayhead deltas. (d) Interpretation of (c). (e) Stacked coarsening-upward sequences in a river-dominated wave-reworked facies association (FA3), overlain by fluvial distributary channel deposits (FA4). Note the tabular geometries and how this differs from the lack of clear bed boundaries and gradual coarsening-upward sequence of Figure 3d. Logged section is SW_38 in Van Yperen, Holbrook, et al. (2019). (f) Example of key stratigraphic surfaces separating coarsening- and fining-upward packages in the distal zone. (g) Outcrop photograph of fluvial distributary channels (FA4) in erosional contact with delta-front sand deposits (FA3). (h) Interpretation of (g), with compensationally stacked mouth bars based on the presence of lensoid-bar geometries. MRS, maximum regressive surface; RCS, Regional composite scour; BDCS, basal distributary composite scour; Triangles indicate grain size trend. (a, b, d, e, f) modified from Van Yperen, Holbrook, et al. (2019)

TABLE 2 Slope and backwater results for trunk channels based on empirical Equation (1). Backwater lengths vary between 71 and 117 km

	D_{50} (mm)	D_{50} (m)	Bankfull flow depth (m)	Half bankfull depth (m)	Slope	Backwater length (km)
Corazon Hill #1	0.28	0.00028	11	5.5	0.000155	71
Canadian River #1 (=HWY 120)	0.17	0.00017	11	5.5	0.000094	117
CR C51A #1	0.23	0.00023	11	5.5	0.000128	86
Red Tounge Mesa #1	0.22	0.00022	11	5.5	0.000122	90

(FA2, FA3, Table 1; Van Yperen, Holbrook, et al., 2019; Van Yperen et al., 2020). The basal surface of the upper Mesa Rica (Figures 5c and 6b,c) separates fluvial sandstones (FA4) of single-story trunk channels (channel type II) and isolated distributary channels (channel type III) from underlying interdistributary fines (FA6) throughout the study area, except in the updip reaches of the proximal zone, where the lower and upper Mesa Rica merge (Holbrook, 2001) (Figure 6).

7.2.2 | Interpretation

The composite basal surface in the proximal zone is the expression of the regional sequence boundary RCS3.1 (SB3.1 in Scott et al., 2004; Oboh-Ikuenobe et al., 2008) and relates to late Albian – early Cenomanian forced regression (Holbrook, 1996, 2001; Holbrook & Wright Dunbar, 1992; Oboh-Ikuenobe et al., 2008; Scott et al., 2004). The basal surface of dispersed single-story trunk channel deposits (channel type II) in the transitional zone, and the erosional composite surfaces bounding the incised-valley fills (channel type IV) in the transitional and distal zones, are all interpreted as different expressions of the RCS3.1 regional sequence-bounding scour (Figure 6c). Several studies have demonstrated that the erosional composite surface that bounds incised-valley fills (channel type IV) is diachronous along strike (Holbrook & Bhattacharya, 2012; Martin et al., 2011; Strong & Paola, 2008) and down dip

(e.g. Holbrook & Bhattacharya, 2012). This insight forms the conceptual base for the Regional Composite Scour, which forms by progradation and scouring of fluvial systems above marine strata, and expands laterally and seaward throughout the transgressive/regressive cycle (Holbrook & Bhattacharya, 2012). The incised-valley walls were shaped continuously and there was continuous deposition during relative sea-level fall. This contradicts non-deposition during valley formation as often suggested (e.g. Van Wagoner et al., 1988). The RCS3.2 (SB3.2 in e.g. Scott et al., 2004; Oboh-Ikuenobe et al., 2008) represents a regional surface as well (Figure 6c) and relates to a second regressive phase of the Mesa Rica system.

7.3 | Basal distributary composite scour

7.3.1 | Description

Erosional composite scours bound sheets of amalgamated distributary-channel deposits (channel type V) in the distal zone (Figures 5f, 6c, 7g,h). They mark sharp facies boundaries that represent the culmination of the typical shallowing-upward character of the deltaic succession. However, newly visited localities (Figure 2) in the distal zone show places where distributary channel deposits are absent and upper delta-front deposits (FA2, FA3) are locally preserved.

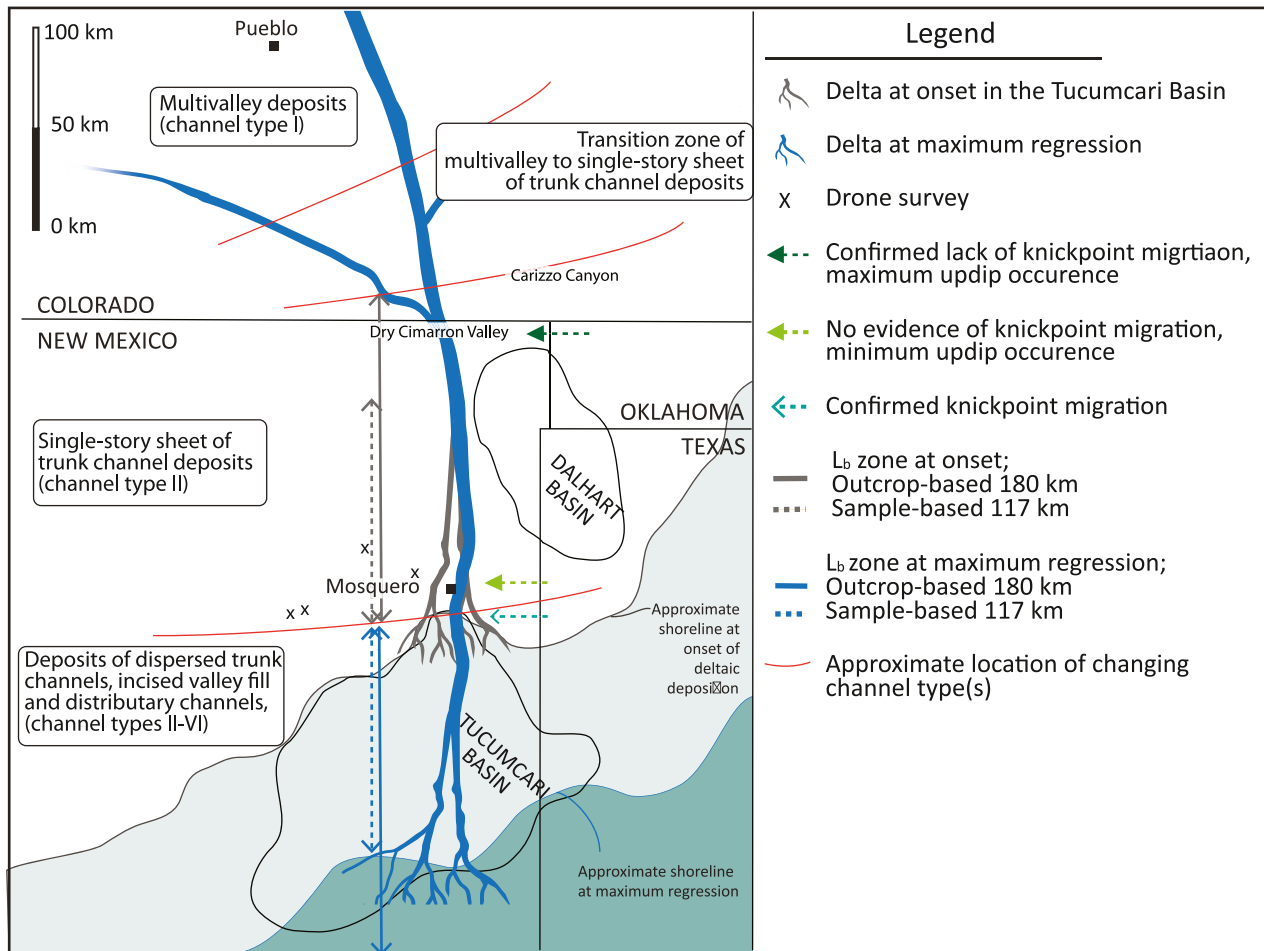


FIGURE 8 Map of study area showing the occurrence of the different channel types (Figure 5), estimated backwater lengths and up-dip knickpoint migration (i.e. upstream limit of valley incision). The river pathway reflects a schematic representation of the depositional system (lower Mesa Rica) at onset of deltaic deposition in the Tucumcari basin (grey) and during maximum regression (blue). Backwater length (L_b) migrates downstream in response to progradation of the lower Mesa Rica delta. The backwater lengths are different depending on the data set (i.e. outcrop- or sample-based)

7.3.2 | Interpretation

Basal composite scours bound distributaries that are younger than the deltaic deposits they incise, and which fed a more distal part of the delta system. These scours form a surface named *basal distributary composite scour (BDCS)*; Figure 6c; Van Yperen, Holbrook, et al., 2019). However, the deposits they bound are localized to discrete deltaic localities and consequently they are not part of the regional scour surface, which is formed by larger channel cut-and-fill-cycles and forms the regional sequence-bounding scour (Van Yperen, Holbrook, et al., 2019). The *basal distributary composite scour* is interpreted to have rather formed by the autogenic process of distributary-channel avulsion and deposition. Such autogenic surfaces commonly have limited lateral extent (Morshedian, MacEachern, Dashtgard, Bann, & Pemberton, 2019), and their recognition is quite uncommon (Pattison, 2018).

8 | BACKWATER LENGTH AND PALEOSLOPE CALCULATIONS

In order to investigate the potential backwater effects on surface generation and down-dip changes in depositional architecture, it is key to establish the landward limit of this marine influence. To do so, we distinguish two datasets for the backwater length calculations in this study: sample-based estimates and outcrop-based estimates. Sample-based estimates provide backwater lengths resulting from empirical Equation (1) using the grain-size samples representative for the coarsest material transported as bedload within trunk rivers (Holbrook & Wanas, 2014; Trampush et al., 2014). Outcrop-based estimates are inferred from changes in fluvial architectural style observed in the studied outcrop profile, and hence a direct measurement within the basin.

Median grain-size values (D_{50}) for four trunk channel-fills (channel type II) of the lower Mesa Rica were derived from

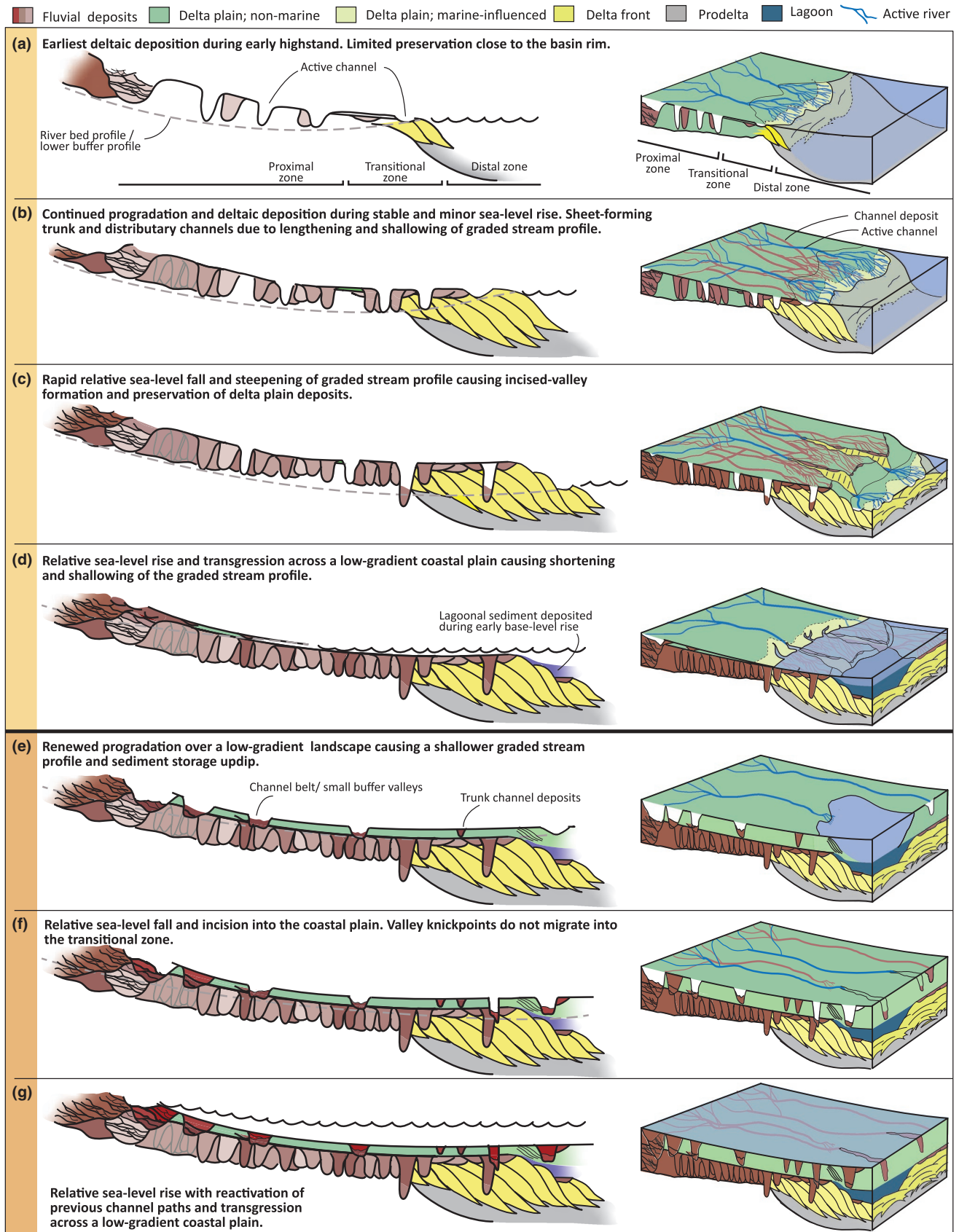


FIGURE 9 Stepwise evolutionary model for the Mesa Rica depositional system. The profile represents a simplified version of the correlation through the study area (Figure 6). The block diagram represents the interpreted depositional model. See text for further discussion

cumulative grain-size distribution curves. They have a D_{50} grain-size value of 0.17–0.28 mm, which fall within the fine sand category (0.125–0.25 mm). We consider a bankfull

depth of 11 m as representative for the trunk channel deposits (channel type II) in the lower Mesa Rica (Holbrook, 1996). This gives one-half bankfull depth of 5.5 m. Using empirical

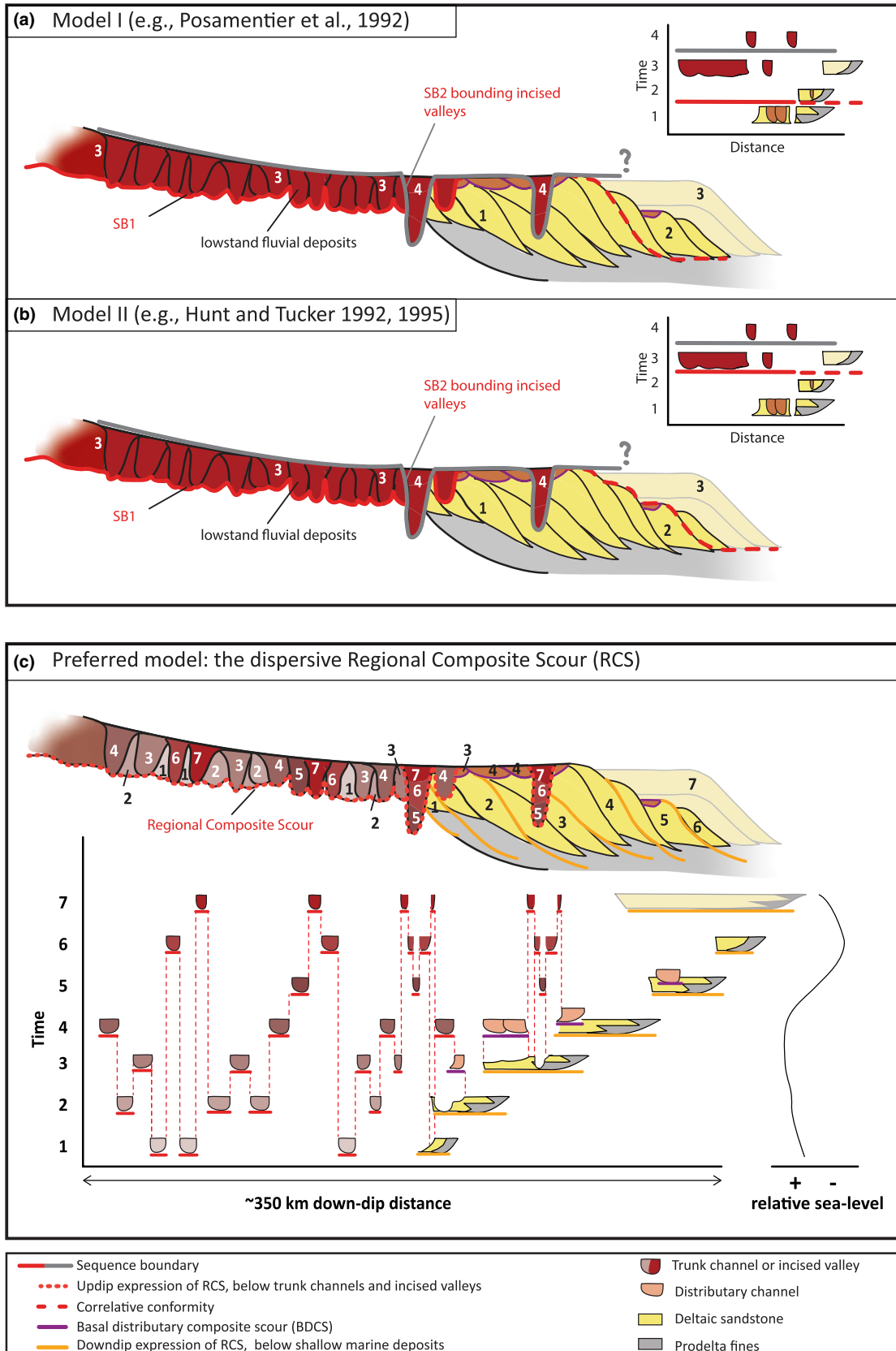


FIGURE 10 (a, b) Simplified depositional profile illustrating different possible sequence stratigraphic correlations between the fluvial and marine realm. Numbers indicate relative time relationships. Both models focus on the sequence boundary (SB)/Regional Composite Scour (RCS) and its marine extent. Model I extends the SB below the first downstepping deltaic deposits as a correlative conformity (Posamentier et al., 1992). Model II extends the SB beneath the lowstand deposits of the last downstep (Hunt & Tucker, 1992, 1995). Both Wheeler diagrams show that there is limited temporal or genetic relationship between the fluvial and deltaic deposits. Labels 'SB1' and 'SB2' are only meant to illustrate chronological order and do not relate to the nomenclature of the identified sequence boundaries of the Mesa Rica depositional system in New Mexico and Colorado (Figure 2b). (c) Simplified depositional profile and Wheeler diagram showing the dispersive nature of the Regional Composite Scour (RCS) in the marine realm. Discrete parts of the composite, highly diachronous and amalgamated erosional composite surface below the fluvial deposits in the proximal zone, are time-equivalent to individual regressive marine surfaces. Each segment of the RCS is contemporaneous to the clinoform surface underlying the genetically-related clinothem. Similarly, segments of the composite scour bounding an incised valley are formed contemporaneously with deposition in the valley, trunk channel deposition in the proximal zone, and clinothem deposition in the distal zone. The regional composite scour is generated in the fluvial realm throughout the T-R cycle. Therefore there is no single correlatable surface in the marine realm, but rather multiple, dispersed segments. Faded deltaic wedges t3 (in a, b) or t7 (in c) are not documented in this study. See text for further discussion

Equation (1), resultant paleoslopes are 0.9×10^{-4} – 1.6×10^{-4} (Table 2). Sample-based estimates of backwater lengths are consequently 71–117 km, which places the maximum backwater length ~30 km south of the New Mexico–Colorado border at onset of deltaic deposition in the Tucumcari basin (Table 2; Figure 8).

Outcrop-based estimates indicate a backwater length of ~180 km, which is the distance between the rim of the Tucumcari basin and the most updip evidence of backwater conditions (Carizzo Canyon, Figure 8). The latter is inferred from the updip limit of single-story trunk channel deposits (channel type II) forming a laterally continuous and extensive sheet. This occurrence is taken as evidence for deposition within the updip reaches of the backwater zone (e.g. Chatanantavet et al., 2012; Jerolmack & Swenson, 2007). Farther updip, the presence of multivalley deposits formed by smaller (likely tributary) channel-fill elements indicate incision and aggradation independent of relative sea-level changes and suggest deposition updip of backwater influences (Figures 5 and 8; e.g. Blum et al., 2013).

The outcrop-based estimate of the backwater length (~180 km) is significantly longer than the sample-based backwater length range of 71–117 km. This mismatch between the two different datasets can be explained by one or a combination of the following reasons: (a) the channels in the most updip evidence of backwater conditions (Carrizzo Canyon) fed a shoreline farther upstream that predates regression to the rim of the Tucumcari Basin. (b) Errors in slope estimates up to a factor 2 are intrinsic to the used calculation method (Holbrook & Wanas, 2014); therefore, outcrop-inferred estimates would be within the error range of the sample-based calculations. (c) Increased avulsion started up dip of the calculated backwater length. We cannot further eliminate uncertainties based on the limited grain-size samples, the studied outcrop profile or the state-of-the-art for backwater calculations.

Backwater length calculations can also be used to estimate the position of the maximum regressive shoreline. This is done by taking the most downdip occurrence of sheet-forming single-story trunk channel deposits (channel

type II) and assume that this position approximates the updip reach of the backwater length at times of maximum regression. The sheet-forming single-story trunk channel deposits disperse around the basin rim, which implies that the upstream limit of the coeval backwater zone was close to this location. Based on this, shoreline progradation made it as far as ~117 km (sample-based) or ~180 km (outcrop-based) south of the basin rim, a position beyond the outcrop window (Figure 8).

9 | INCISED VALLEYS: PALEOFLOW DEPTHS AND KNICKPOINT MIGRATION

Incised valleys form where regression exposes a slope steeper than the contemporary river equilibrium profile, and have been interpreted to evidence relative sea-level fall (e.g. Blum et al., 2013; Catuneanu, 2006; Posamentier et al., 1988; Van Wagoner et al., 1988). Consequently, their adequate recognition influences the understanding of a depositional system. In the Mesa Rica system, incised-valley fills (channel type IV) are on average 16 m thick in the transitional zone. Bankfull paleo-flow depth (Allen, 1982; Best & Fielding, 2019; Bradley & Venditti, 2017) of average channel fills within these valleys was ~7.4 m, based on cross strata thicknesses and mean dune height calculations (Leclair & Bridge, 2001). This indicates that valleys were cut by channels that had undergone approximately two bifurcations (Yalin, 1992), or they were initially smaller because they carried less discharge than the largest trunk channels. Their water surface was 8.6 meter below the topographic surface (16 m valley depth minus 7.4 m depth of active channel). In the distal zone, complete incised-valley fills are on average 11 m thick. Applying the same method, their average channel story thickness within these valley scours is ~5.9 m. Consequently, their water surface was ~5.1 m below the concurrent topographic surfaces.

The updip extent of valley incision relates to updip knickpoint migration over time (Posamentier & Vail, 1988; Wescott, 1993). The dataset allows estimates for both minimum and

maximum updip occurrence of knickpoints. The maximum updip occurrence is inferred from extensive mapping and architectural-element analysis just south of the Colorado–New Mexico border (i.e. Dry Cimarron Valley in Holbrook, 1996). Here, incised-valley deposits are absent which confirms the lack of knickpoint migration to this distance up dip (Figure 8). The minimal updip occurrence of knickpoint incision is the southernmost location without any valleys observed and hence no evidence for knickpoint migration (Figure 8). However, this is based on local sampling of discontinuous outcrops with drone surveys and not the systematic examination of continuous outcrops executed further north. The localized nature of this dataset (Figure 8) leaves room for incised-valley deposits missed by drone coverage. The resultant range between the minimum and maximum updip occurrence of valley knickpoints is approximately 115 km.

The maximum updip occurrence of valley knickpoints is situated in between the sample-based and outcrop-based backwater lengths at onset of deltaic deposition in the Tucumcari Basin (Figure 8). During maximum regression, the maximum updip occurrence of valley knickpoints scales to $\sim 2\times$ the backwater length from the maximum regressive shoreline (Figure 8). This scaling relationship is used to discuss the forcing mechanism for these large erosional surfaces (see Section 10; Fernandes et al., 2016; Ganti et al., 2019; Lamb et al., 2012; Trower et al., 2018).

10 | DISCUSSION

10.1 | Relative sea-level control on depositional architecture

Evidence for relative sea-level fall during deposition of the Mesa Rica system is threefold: (a) downstepping delta-front geometries in the distal zone (Figure 6b); (b) key stratigraphic surfaces (MRS1, MRS2) extend over regional distances (>300 km, Figure 6c), which cannot be explained solely by autogenic behaviour (Van Yperen, Holbrook, et al., 2019); (c) multi-storey sandstone bodies (channel type IV, Figure 5d,e) represent incised valleys, based on their regional occurrence, their multi-storey and multi-lateral infill, and their estimated channel incisions at least two channel depths below the concurrent topography (Fielding, 2008; Holbrook, 2001; Martin et al., 2011; Strong & Paola, 2008; Van Yperen, Holbrook, et al., 2019). Flume modelling results show improbable autogenic formation of multi-storey sandstone bodies with more than two channel depths (Strong & Paola, 2008). Despite all this, a potential other scenario for autogenic multi-storey sandstone body generation is the scouring by trunk channels and later reoccupation and deposition by distributaries, creating a multi-storey infill. However, the coeval downstepping delta front geometries in the Mesa Rica evidence an externally-forced drop in sea level (Van Yperen, Holbrook, et al.,

2019). This, and concurrence with the incised-valley scours, is conclusive for a fall in relative sea level.

The sea-level drop needed for the formation of the documented valleys in the lower Mesa Rica is ~ 9 m. This is based on average bankfull channel depths of 7.4 m within the 16-m-thick valleys, which implies that their water surfaces had dropped ~ 9 m. The subsequent transgression covered a distance of roughly 250 km, based on the occurrence of paralic middle Mesa Rica deposits in the distal reaches of the proximal zone (Figure 6b) and the reconstruction of weak brackish influence in southern Colorado (Oboh-Ikuenobe et al., 2008). The estimated minimum and maximum slopes values for the single story trunk channels of 0.9×10^{-4} and 1.6×10^{-4} would have required a relative sea-level rise between 23 and 40 m, to cause this flooding, respectively. In addition to the ~ 9 m sea-level drop this means a total of 32 to 49 m rise in relative sea-level is likely for flooding of the lower Mesa Rica system.

10.2 | A stepwise model for the Mesa Rica depositional system

In the lower Mesa Rica, multivalley deposits (channel type I) appear ~ 240 km upstream from the Tucumcari basin rim, which equals $\sim 2\times$ the sample-based maximum backwater length (i.e. 117 km), and $\sim 1.5\times$ the outcrop-based backwater length (i.e. 180 km). The multivalley deposits thin downstream to a single-story-thick channel sheet (channel type II; Figures 5 and 6a,b) which also thins towards the rim of the marine basin. This is consistent with the anchoring of the graded stream profiles, causing convergence of the upper and lower buffer profiles (Figure 1b; Holbrook et al., 2006) accompanied with vertical limits on aggradation and incision (e.g. Holbrook et al., 2006; Mackin, 1948; Quirk, 1996). Channel thinning in the transitional and distal zones results from repetitive bifurcation (Edmonds & Slingerland, 2007; Yalin, 1992). Onset of deltaic deposition occurred close to the rim of the basin (Figure 9a). However, low-accommodation conditions limited the preservation of deltaic sediments, as younger prograding fluvial channels were forced to use the same accommodation (Figure 9b). Consequently, these channels almost completely eroded the deposits that recorded the facies change from shallow-marine to fluvial settings, which is now preserved as a rather abrupt transition. Thickness values of the delta-front deposits suggest water depth abruptly increased basinwards in the transitional and distal zones (Figure 9b). Here, single-story trunk channels and incised valleys (channel type II and IV, Figure 5) incise locally into underlying delta front strata or distributary-channel deposits (channel type V; Figure 9b). Basal surfaces of these sheet-forming distributary-channel deposits (*basal distributary composite scour*) eroded most upper delta-front

sediment and indicate that accommodation was still limited. The single-story trunk channel elements (channel type II) were deposited during continued normal progradation and feed a more distal part of the delta. Later forced regression and progressively less accommodation resulted in downstepping delta-front geometries (Figure 9c). Subsequently, this fall in relative sea level caused valley incision (channel type IV) as the equilibrium profile adjusted to steeper gradients (Figure 9c; e.g. Talling, 1998). After a period with steepened depositional gradients, the equilibrium profile shallowed during subsequent relative sea-level rise. Incised valleys filled and facies belts shifted ~250 km landwards, based on the occurrence of paralic middle Mesa Rica deposits in the distal reaches of the proximal zone (Figure 9d), although fully-marine conditions were not established over this entire length (Oboh-Ikuenobe et al., 2008).

Onset of upper Mesa Rica deposition by renewed normal progradation caused fluvial and interdistributary bay deposition (Figure 9e). The main differences with the lower Mesa Rica are two: first, the upper Mesa Rica is characterized by a higher A/S ratio (Figure 6). This can be a consequence of insufficient time to form a sheet of laterally amalgamated channel-fill elements (channel type II), as characteristic for the lower Mesa Rica. Another explanation is a higher profile gradient for the lower Mesa Rica than for the upper Mesa Rica, as the first prograded into the Tucumcari Basin, whilst the latter prograded over a shallower flooding surface (Figure 9e). Such low gradient conditions are accompanied with the relative increase in preservation of delta plain fines. Low profile gradients promoted this preferred upstream deposition of the sand-fraction (Holbrook & Bhattacharya, 2012). Secondly, incised valleys of the upper Mesa Rica formed during a subsequent relative sea-level fall, but their knickpoints did not migrate into the transitional zone (Figure 9f). The genetically related delta front deposits to this down step accumulated beyond the outcrop window and thus away from the study profile.

In general, this model suggests that cut-and-fill cycles of all channel types occurred continuously throughout a relative sea-level cycle, and during deposition of both the lower and upper Mesa Rica. Changes in relative sea level triggered the equilibrium profile to adjust, which in turn determined the vertical limits of erosion and deposition along the lower reaches of the depositional profile.

10.3 | Backwater effects in the Mesa Rica depositional system

The regional scale of the Mesa Rica outcrop profile provides a unique opportunity to study changes in architectural style and their relation to backwater effects. The observation of flood-induced scours up to 3× bankfull depth (Fernandes

et al., 2016; Ganti et al., 2019; Lamb et al., 2012; Trower et al., 2018) poses potential challenges to differentiate large scours induced by drawdown effects in the backwater zone (e.g. Lamb et al., 2012), from allogenic-formed incised-valley fills (e.g. Blum et al., 2013). Trower et al. (2018) showed that maximum scour depths of the Cretaceous Castlegate Sandstone range between 1 and 3× bankfull channel depth, and questioned the role of base-level fall in creating these erosional surfaces. The maximum scour depth of flood-induced erosion is proportional to flow variability in normal-flow depths (Chatanantavet & Lamb, 2014), which is typically 0.5 to 3× bankfull flow depth upstream of their backwater zone (Ganti et al., 2014). Therefore, allogenic scour depths must theoretically *exceed* bankfull flow depth (>3×) and occur over a greater distance than the backwater length in order to unambiguously distinguish allogenic signals from backwater-induced scours (Ganti et al., 2014, 2019; Trower et al., 2018). In our study, incised valleys are on average 11–16 m thick and their infill indicates deposition in 5.1–8.6 m thick channels. Consequently, scouring happened at *less* than 3× below bankfull depth. Nevertheless, the observations that support the existence of a drop in relative sea level listed in the previous section (i.e. the downstepping delta front geometries) suggest these valleys formed as a response to an allogenic-induced steepening of the graded stream profile and not as a consequence to flood-induced scours within the backwater zone. The limited distance over which the knickpoints migrated (~1–2 L_b) and hence the incised valleys occur relates to the minor drop in sea level (~9 m) and a short-lived nature of this relative sea-level drop. The latter is inferred from the narrow incised valleys (indicating limited time for lateral migration or erosion of valley sidewalls), good preservation of delta plain deposits (which would otherwise be cannibalized in this low-accommodation setting), and the knickpoint of these valleys being close the upstream limit of the backwater zone. In summary, one of the main criteria offered by other authors (Ganti et al., 2014, 2019; Trower et al., 2018) to unambiguously assign an allogenic origin to the incised valleys (i.e. occurrence of incised valleys over distances longer than the backwater length and scouring >3× bankfull flow depth) is not consistent with the results of this study, which evidence allogenic forcing of valley scours <3× bankfull flow depth occurring over one to two times the backwater length (~1–2 L_b). This emphasizes that decoupling autogenic and allogenic controls on erosional surface generation might be especially problematic, particularly in low-gradient river systems.

Other down-dip changes often linked to backwater effects are downstream fining channel belt deposits, decrease in sinuosity, and channel belt deepening and narrowing (e.g. Fernandes et al., 2016; Lamb et al., 2012; Martin et al., 2018; Nittrouer, 2013). Of these, this study has only documented channel-belt narrowing, but the lack of other downdip changes

linked to backwater effects in the Mesa Rica system can have several causes. Firstly, backwater analyses of the sedimentary record imply that backwater hydrodynamics must persist long enough for its signal to be recorded (Chatanantavet & Lamb, 2014; Ganti, Chadwick, Hassenruck-Gudipate, & Lamb, 2016). Low-accommodation settings lower preservation potential in general, which might lower the chances of such signals being recorded in addition. Secondly, the generally low preservation potential in low-accommodation systems might lower the chance to record this signal. This might be particularly challenging in low-accommodation systems, where preservation potential is generally low. Secondly, backwater concepts originated and are predominantly tested on the Mississippi river, and supported by numerical models assuming simplified input parameters (e.g. Chatanantavet et al., 2012; Fernandes et al., 2016; Lamb et al., 2012; Nittrouer, 2013; Nittrouer et al., 2012). Consequently, their full applicability in other settings is part of future research. Several other studies have documented results that contrast the 'expected' backwater effects, such as channel widening and shallowing in tide-dominated river deltas (Gugliotta & Saito, 2019), or absence of erosion in the distal part of the backwater zone during river floods (Zheng, Edmonds, Wu, & Han, 2019). The interplay of sediment type, depositional gradient, climate and (above all) time and preservation potential make trends in backwater effects difficult to predict.

10.4 | Sequence stratigraphic correlations in low-accommodation settings

Conceptually, there are several possible scenarios for correlation between fluvial and genetically-related deltaic deposits. One scenario places the sequence boundary below fluvial deposits and extends it below the first downstepping deltaic deposits as a correlative conformity (Figure 10a; e.g. Posamentier, Allen, James, & Tesson, 1992) or to the correlative conformity beneath the lowstand deposit is of the last downstep (Figure 10b; Hunt & Tucker, 1992, 1995). In another scenario, the sequence boundary is correlated with the flooding surface on top of the deltaic strata (Embry, 1995). In both scenarios, the normal-regressive deltaic deposits are included in the highstand systems tract and only late lowstand shallow marine deposits are time equivalent to the fluvial strata. Theoretically, temporal relationships between fluvial and marine strata would be distinctive, as the fluvial facies would gradually transition into deltaic facies in highstand and early falling stage strata. However, in this study, there is an abrupt change from fully-fluvial to deltaic deposits (Figure 6b), and so no true zone with gradational facies transitions is identifiable. But by principle, such facies transition must have been present at least at the onset of deltaic deposition. We argue that this facies transition was eroded at later time, when the

fluvial system advanced over highstand strata and completely eroded the delta deposits to one channel depth up to approximately the northern margin of the Tucumcari Basin (Figure 9a,b). Consequently, the area that theoretically holds the physical evidence for a temporal relationship between fluvial and shallow marine highstand strata is nowadays eroded. This process by which prograding fluvial facies incise and remove the record of underlying highstand deposits is commonly referred to as compensation (Hajek & Straub, 2017; Holbrook & Miall, 2020; Straub & Esposito, 2013). Examples of complete compensation, as happened with lower Mesa Rica deltaic strata, are atypical (Holbrook & Miall, 2020).

Following Posamentier et al. (1992), Hunt and Tucker (1992, 1995) or Embry (1995), an additional fall in relative sea level would be needed to explain the sequence boundary (SB2 in Figure 10a,b) that bounds the incised valleys (channel type IV) and incises into the single-story sheet of trunk channels (channel type III) that in turn is underlain by a sequence boundary (SB1 in Figure 10a,b). As studies on modern fluvio-deltaic also suggest (Blum et al., 2013), our model infers temporal relationships between fluvial and deltaic deposits (Figure 9a–d) and no additional fall in relative sea level is needed (see next section for further discussion).

10.5 | The dispersive nature of the Regional Composite Scour in the marine realm

The extent of the traditional sequence boundary into correlative marine strata is often debated and causes practical problems in its application (e.g. Bhattacharya, 2011; Bhattacharya et al., 2019). The Regional Composite Scour (RCS) acknowledges the three-dimensional and diachronous nature of this surface in the continental realm. This includes along-strike variability, which is crucial to understand any depositional system (e.g. Amorosi et al., 2019; Madof et al., 2016; Martinsen & Helland-Hansen, 1995; Miall, 2015).

In the Mesa Rica system, the nature and predominantly fully fluvial infill of single-story trunk channel deposits (channel type II), incised valley fill (channel type IV) and amalgamated distributary channel deposits (channel type V) imply active filling of channels rather than passive backfilling, and suggests continuous reshaping and active deposition occurred at the delta plain and in incised valleys. Additionally, we mapped and physically traced several stratigraphic surfaces down dip of the Regional Composite Scour (RCS). These are (a) the *Basal Distributary Composite Scour* (BDCS) below amalgamated distributary channel deposits, (b) the basal surface below dispersed trunk channel deposits incising into deltaic deposits, (c) composite surfaces bounding incised valleys, and (d) a downstep in deltaic onlap (Figures 6c and 7). None of them is necessarily equivalent to the sequence boundary as defined originally in the fluvial

realm (e.g. Hunt & Tucker, 1992; Posamentier et al., 1988; Van Wagoner et al., 1988). However, recent understanding of the diachronous character of the sequence boundary/RCS (Holbrook & Bhattacharya, 2012; Martin et al., 2009; Strong & Paola, 2008) entails that individual segments of these stratigraphic surfaces each correlate with discrete parts of the RCS: the RCS was created in the proximal zone throughout the complete relative sea-level cycle, due to ongoing river erosion and virtually contemporaneously deposition within the channel (Figure 9a–d). The sediment that was not incorporated into the updip fluvial deposits bypassed this area and fed the coeval deltaic clinothem in the distal zone. Consequently, each part of the RCS is time-equivalent to the clinoform surface underlying each genetically-related clinothem (Figure 10c).

Thus, the RCS results from multi-phase scouring throughout a relative sea-level cycle (Holbrook & Bhattacharya, 2012; Martin et al., 2009; Strong & Paola, 2008), contemporaneous to deposition in the shallow-marine realm. The composite nature of the RCS and the documented and physically traced stratigraphic surfaces evidence that the fluvial regional composite scour disperses into several surfaces in the shallow-marine part of the depositional system, rather than one single, correlatable surface. This also implies that no third-order sequence boundaries are necessary to correlate the incised valleys with the delta-front sandstones they incise into (Pattison, 2019). Dispersive key stratigraphic surfaces have been documented previously (Korus & Fielding, 2017). In their study, composite sequence boundaries split in down-dip direction and are physically traceable as they pass into conformable surfaces. This differentiates from the dispersion of a single sequence boundary into several surfaces as highlighted in our study.

The application of this concept along a complete fluvio-deltaic system evidences the need to focus on dynamics and mechanisms creating key sequence stratigraphic surfaces, rather than debating their nomenclature or chronostratigraphic value. This debate seems an impossible quest for a single correlatable surface in the marine realm, given that regional composite scours may be generated in the fluvial realm throughout a relative sea-level cycle. Additionally, the active deposition and continuous reshaping of channels and incised valleys suggests that erosion and deposition occurred virtually contemporaneous at any point along the depositional profile, which implies that there is also no complete bypass at any given time or point in the system. This cautions against many stratigraphic models in which low-accommodation settings are interpreted to promote complete bypass, especially during forced regression, which results in extensive lowstand wedges (e.g. Emery & Myers, 2009; Posamentier et al., 1988). Results of this study suggest that sediment is stored more continuously in the fluvial part of depositional systems than conventional

models suggest. Basin reconstructions and source-to-sink analysis need to take this into account in order to adequately resolve the amount of sediment volume trapped temporally or permanently in the system throughout a complete relative sea-level cycle.

11 | CONCLUSIONS

- This work presents for the first time a regional-scale (~400 km) and depositional-dip parallel stratigraphic correlation of the low-accommodation Mesa Rica fluvio-deltaic system, and illustrates the complexities inherent to sequence stratigraphic interpretations of fluvial to marine systems.
- The distribution, stacking patterns and dimensions of six distinguished channel types (i.e. multivalley-sheet, single story-sheet of trunk channels, isolated fluvial distributary channels and channel belts, incised valley, fluvial distributary-channel sheet, marine-influenced distributary channel) reflect their position along the equilibrium profile and a general trend of decreasing accommodation towards the paleoshoreline.
- Evidence for relative sea-level fall during deposition of the Mesa Rica system is based on downstepping delta-front geometries in the distal zone, key stratigraphic surfaces extending over regional distances, and the regional occurrence of valley incised valley scours that correlate with the downstepping delta-front strata.
- Incised valley scours <3× bankfull flow depth occurring over one to two times the backwater length (~1–2 L_b) resulted from allogenic-induced steepening of the graded stream profile and not as a consequence of flood-induced scouring in the backwater zone, as other authors have suggested. Even though decoupling autogenic and allogenic controls on erosional surface generation might be problematic, particularly in low-gradient river systems, it is better to differentiate flood-induced multi-storey channels from allogenic-formed incised-valley fills based on multiple observations rather than only scour depth and occurrence over a distance compared to backwater length.
- The position of changing fluvial architecture from multivalley to single story channel fill deposits and the distance over which incised valley scour scale with ~1–2 backwater lengths (L_b). Within the backwater zone however, only limited changes in fluvial architecture observed in the Mesa Rica system (i.e. channel belt narrowing) fit the general model for backwater-mediated down-dip changes. This can be related to backwater hydrodynamics not persisting long enough for its signal to be recorded, and/or to their limited preservation potential in low-accommodation systems.

- The fluvial Regional Composite Scour (RCS) is the result of multi-phase channel scouring throughout a relative sea-level cycle, and disperses into several surfaces in the shallow-marine strata, rather than forming one single, correlatable surface. Each segment of the RCS is contemporaneous to discrete elements of these correlative sub-regional stratigraphic surfaces, i.e. the basal surface below dispersed trunk channels incising into deltaic deposits, the Basal Distributary Composite Scour (BDSC) bounding laterally amalgamated distributary channels, erosional composite surfaces bounding incised valleys, and the clinof orm surface underlying the genetically-related clinof orm. Only the latter two are traditionally considered a continuation of the sequence boundary.
- Low-accommodation settings do not necessarily promote complete bypass and sediment can be stored continuously in the fluvial part of depositional systems. This has important implications for the amount of sediment volume trapped temporally or permanently in the system throughout a complete relative sea-level cycle, and should therefore be considered in basin reconstructions and source-to-sink analysis.

ACKNOWLEDGEMENTS

The Lower Cretaceous basinal studies of the Arctic (LoCra) consortium and the Research Centre for Arctic Petroleum Exploration (ARCEX) allocated funding for field expeditions. Associate Editor Cari Johnson and reviewers Brian Willis, Nigel Mountney and Chris Fielding are thanked for their constructive criticism of this article. Sincere thanks go to Lina Hedvig Line, Blake Warwick and Edwin Tieman for field-assistance. We thank Gretchen Gurtler and Axel Hungerbuehler from the Mesalands Dinosaur Museum and Natural Sciences Laboratory in Tucumcari for irreplaceable logistical help. Last but definitely not least, we thank the Trigg family, the Mackecknie family and many others in the Harding, San Miguel and Quay counties for their hospitality and permitting us access to their property, with a special thanks to Sally, Kristen, Rick and Tom.

CONFLICT OF INTEREST


There are no conflicts of interest for any of the authors in the preparation or publication of this work.

DATA AVAILABILITY STATEMENT

The data that support the findings of this study are available from the corresponding author upon reasonable request.

ORCID

Anna E. van Yperen  <https://orcid.org/0000-0003-3703-2754>

Miquel Poyatos-Moré  <https://orcid.org/0000-0001-7813-8868>

Ivar Midtkandal  <https://orcid.org/0000-0002-4507-288X>

REFERENCES

- Ainsworth, R. B., Vakarelov, B. K., MacEachern, J. A., Rarity, F., Lane, T. I., & Nanson, R. A. (2017). Anatomy of a shoreline regression: Implications for the high-resolution stratigraphic architecture of deltas. *Journal of Sedimentary Research*, 87, 425–459. <https://doi.org/10.2110/jsr.2017.26>
- Allen, J. R. L. (1982). Empirical character of ripples and dunes formed by unidirectional flows. In J. R. L. Allen (Ed.), *Sedimentary structures: Their character and physical basis, developments in sedimentology* (pp. 307–344). Amsterdam: Elsevier.
- Amorosi, A., Bruno, L., Campo, B., Costagli, B., Dinelli, E., Hong, W., ... Vaiani, S. C. (2019). Tracing clinof orm geometry and sediment pathways in the prograding Holocene Po Delta system through integrated core stratigraphy. *Basin Research*, 32, 206–215. <https://doi.org/10.1111/bre.12360>
- Amorosi, A., Maselli, V., & Trincardi, F. (2016). Onshore to offshore anatomy of a late Quaternary source-to-sink system (Po Plain-Adriatic Sea, Italy). *Earth-Science Reviews*, 153, 212–237. <https://doi.org/10.1016/j.earscirev.2015.10.010>
- Aschoff, J. L., Olariu, C., & Steel, R. J. (2018). Recognition and significance of bayhead delta deposits in the rock record: A comparison of modern and ancient systems. *Sedimentology*, 65, 62–95. <https://doi.org/10.1111/sed.12351>
- Bagnold, R. A. (1977). Bed-load transport by natural rivers. *Water Resources Research*, 13, 303–312. <https://doi.org/10.1029/WR013i002p00303>
- Beerbower, J. R. (1964). Cyclothem and cyclic depositional mechanisms in alluvial plain sedimentation. In D. F. Merriam (Ed.), *Symposia on cyclic sediments* (Vol. 169, pp. 31–42). Kansas: Kansas Geological Survey.
- Best, J., & Fielding, C. R. (2019). Describing fluvial systems: Linking processes to deposits and stratigraphy. *Geological Society, London, Special Publications*, 488, 152–166. <https://doi.org/10.1144/SP488-2019-056>
- Bhattacharya, J. P. (2010). Deltas. In N. P. James & R. W. Dalrymple (Eds.), *Facies models 4* (pp. 233–264). Geological association of Canada.
- Bhattacharya, J. P. (2011). Practical problems in the application of the sequence stratigraphic method and key surfaces: Integrating observations from ancient fluvial-deltaic wedges with Quaternary and modelling studies. *Sedimentology*, 58, 120–169. <https://doi.org/10.1111/j.1365-3091.2010.01205.x>
- Bhattacharya, J. P., Miall, A. D., Ferron, C., Gabriel, J., Randazzo, N., Kynaston, D., ... Singer, B. S. (2019). Time-stratigraphy in point sourced river deltas: Application to sediment budgets, shelf construction, and paleo-storm records. *Earth-Science Reviews*, 199, 102985. <https://doi.org/10.1016/j.earscirev.2019.102985>
- Blakey, R. C. (2014). Paleogeography and paleotectonics of the Western Interior Seaway, Jurassic-Cretaceous of North America. *Search and Discovery*, Article, no. 30392, 72 pp.
- Blum, M., Martin, J., Milliken, K., & Garvin, M. (2013). Paleovalley systems: Insights from Quaternary analogs and experiments. *Earth-Science Reviews*, 116, 128–169. <https://doi.org/10.1016/j.earscirev.2012.09.003>
- Bradley, R. W., & Venditti, J. G. (2017). Reevaluating dune scaling relations. *Earth Science Reviews*, 165, 356–376. <https://doi.org/10.1016/j.earscirev.2016.11.004>
- Bridge, J. S., & Tye, R. S. (2000). Interpreting the dimensions of ancient fluvial channel bars, channels, and channel belts from wireline-logs and cores. *AAPG bulletin*, 84(8), 1205–1228.

- Broadhead, R. F. (2004). Petroleum geology of the Tucumcari Basin – Overview and recent exploratory activity. *New Mexico Geology*, 26, 90–94.
- Catuneanu, O. (2006). *Principles of sequence stratigraphy*. Amsterdam: Elsevier.
- Chatanantavet, P., & Lamb, M. P. (2014). Sediment transport and topographic evolution of a coupled river and river plume system: An experimental and numerical study. *Journal of Geophysical Research: Earth Surface*, 119, 1263–1282. <https://doi.org/10.1002/2013JF002810>
- Chatanantavet, P., Lamb, M. P., & Nittrouer, J. A. (2012). Backwater controls of avulsion location on deltas. *Geophysical Research Letters*, 39, <https://doi.org/10.1029/2011GL050197>
- Chow, V. T. (1959). *Open-channel hydraulics*. New York: McGraw-Hill.
- Chumakov, N. M., Zharkov, M. A., Herman, A. B., Doludenko, M. P., Kalandadze, N. N., Lebedey, E. L., & Rautian, A. S. (1995). Climatic belts of the mid-Cretaceous time. *Stratigraphy and Geological Correlation*, 3, 42–63.
- Colombera, L., Shiers, M. N., & Mountney, N. P. (2016). Assessment of backwater controls on the architecture of distributary-channel fills in a tide-influenced coastal-plain succession: Campanian Neslen formation, U.S.A. *Journal of Sedimentary Research*, 86, 1–22. <https://doi.org/10.2110/jsr.2016.33>
- DeCelles, P. G. (2004). Late Jurassic to Eocene evolution of the Cordilleran thrust belt and foreland basin system, western U.S.A. *American Journal of Science*, 304, 105–168. <https://doi.org/10.2475/ajs.304.2.105>
- Edmonds, D. A., & Slingerland, R. L. (2007). Mechanics of river mouth bar formation: Implications for the morphodynamics of delta distributary networks. *Journal of Geophysical Research: Earth Surface*, 112, 1–14. <https://doi.org/10.1029/2006JF000574>
- Embry, A. F. (1995). Sequence boundaries and sequence hierarchies: Problems and proposals. In R. J. Steel, V. L. Felt, E. P. Johannessen, C. Mathieu (Eds.), *Sequence stratigraphy on the Northwest European Margin* (Vol. 5, pp. 1–11). Stavanger, Norway: Norwegian Petroleum Society.
- Emery, D., & Myers, K. (2009). *Sequence stratigraphy*. Oxford: Blackwell Science.
- Fernandes, A. M., Törnqvist, T. E., Straub, K. M., & Mohrig, D. (2016). Connecting the backwater hydraulics of coastal rivers to fluvio-deltaic sedimentology and stratigraphy. *Geology*, 44, 979–982. <https://doi.org/10.1130/G37965.1>
- Fielding, C. R. (2008). Sedimentology and stratigraphy of large river deposits: Recognition in the ancient record, and distinction from Incised Valley Fills. In A. Gupta (Ed.), *Large rivers: Geomorphology and managements* (pp. 97–113). John Wiley & Sons.
- Flemming, B. W. (2000). *The role of grain size, water depth and flow velocity as scaling factors controlling the size of subaqueous dunes: Marine Sandwave Dynamics*. Proceedings of and International Workshop (pp. 55–60).
- Ganti, V., Chadwick, A. J., Hassenruck-Gudipate, H. J., & Lamb, M. P. (2016). Avulsion cycles and their stratigraphic signature on an experimental backwater-controlled delta. *Journal of Geophysical Research: Earth Surface*, 121, 1651–1675. <https://doi.org/10.1002/2016JF003915>
- Ganti, V., Chu, Z., Lamb, M. P., Nittrouer, J. A., & Parker, G. (2014). Testing morphodynamic controls on the location and frequency of river avulsions on fans versus deltas: Huanghe (Yellow River), China. *Geophysical Research Letters*, 41, 7882–7890. <https://doi.org/10.1002/2014GL061918>
- Ganti, V., Lamb, M. P., & Chadwick, A. J. (2019). Autogenic erosional surfaces in fluvio-deltaic stratigraphy from floods, avulsions, and backwater hydrodynamics. *Journal of Sedimentary Research*, 89, 815–832. <https://doi.org/10.2110/jsr.2019.40>
- Gugliotta, M., & Saito, Y. (2019). Matching trends in channel width, sinuosity, and depth along the fluvial to marine transition zone of tide-dominated river deltas: The need for a revision of depositional and hydraulic models. *Earth-Science Reviews*, 191, 93–113. <https://doi.org/10.1016/j.earscirev.2019.02.002>
- Hack, J. T. (1973). Stream-profile analysis and stream-gradient indices. *U.S. Geological Survey, Journal of Research*, 1, 421–429.
- Hajek, E. A., & Straub, K. M. (2017). Autogenic sedimentation in clastic stratigraphy. *Annual Review of Earth and Planetary Sciences*, 45, 681–709. <https://doi.org/10.1146/annurev-earth-063016-015935>
- Hodgson, D. M., Kane, I. A., Flint, S. S., Brunt, R. L., & Ortiz-Karppf, A. (2016). Time-transgressive confinement on the slope and the progradation of basin-floor fans: Implications for the sequence stratigraphy of deep-water deposits. *Journal of Sedimentary Research*, 86, 73–86. <https://doi.org/10.2110/jsr.2016.3>
- Holbrook, J. M. (1996). Complex fluvial response to low gradients at maximum regression; a genetic link between smooth sequence-boundary morphology and architecture of overlying sheet sandstone. *Journal of Sedimentary Research*, 66, 713–722. <https://doi.org/10.1306/D42683EC-2B26-11D7-8648000102C1865D>
- Holbrook, J. M. (2001). Origin, genetic interrelationships, and stratigraphy over the continuum of fluvial channel-form bounding surfaces: An illustration from middle Cretaceous strata, Southeastern Colorado. *Sedimentary Geology*, 144, 179–222. [https://doi.org/10.1016/S0037-0738\(01\)00118-X](https://doi.org/10.1016/S0037-0738(01)00118-X)
- Holbrook, J. M., & Bhattacharya, J. P. (2012). Reappraisal of the sequence boundary in time and space: Case and considerations for an SU (subaerial unconformity) that is not a sediment bypass surface, a time barrier, or an unconformity. *Earth-Science Reviews*, 113, 271–302. <https://doi.org/10.1016/j.earscirev.2012.03.006>
- Holbrook, J., & Miall, A. D. (2020). Time in the rock: A field guide to interpreting past events and processes from a fragmentary siliciclastic archive. *Earth-Science Reviews*, 203, 103121. <https://doi.org/10.1016/j.earscirev.2020.103121>
- Holbrook, J. M., Scott, R. W., & Oboh-Ikuenobe, F. E. (2006). Base-level buffers and buttresses: A model for upstream versus downstream control on fluvial geometry and architecture within sequences. *Journal of Sedimentary Research*, 76, 162–174. <https://doi.org/10.2110/jsr.2005.10>
- Holbrook, J. M., & Wanas, H. (2014). A fulcrum approach to assessing source-to-sink mass balance using channel paleohydrologic parameters derivable from common fluvial data sets with an example from the Cretaceous of Egypt. *Journal of Sedimentary Research*, 84, 349–372. <https://doi.org/10.2110/jsr.2014.29>
- Holbrook, J. M., & White, D. C. (1998). Evidence for subtle uplift from lithofacies distribution and sequence architecture: Examples from lower Cretaceous strata of northeastern. In K. W. Shanley & P. J. McCabe (Eds.), *Relative role of eustasy, climate, and tectonism in continental rocks* (pp. 123–132). New Mexico: SEPM Special Publication.
- Holbrook, J. M., & Wright Dunbar, R. (1992). Depositional history of Lower Cretaceous strata in northeastern New Mexico: Implications for regional tectonics and depositional sequences. *Geological Society of America Bulletin*, 104, 802–813. [https://doi.org/10.1130/0016-7606\(1992\)104<0802](https://doi.org/10.1130/0016-7606(1992)104<0802)
- Holbrook, J. M., Wright, R., & Kietzke, K. K. (1987). Stratigraphic relationships at the Jurassic-Cretaceous boundary in east-central

- New Mexico. In S. G. Lucas & A. P. Hunt (Eds.), *Northeastern New Mexico. New Mexico geological society, guidebook, 38th Field Conference* (pp. 161–165).
- Hunt, D., & Tucker, M. E. (1992). Stranded parasequences and the forced regressive wedge systems tract: Deposition during base-level fall. *Sedimentary Geology*, *81*, 1–9. [https://doi.org/10.1016/0037-0738\(92\)90052-S](https://doi.org/10.1016/0037-0738(92)90052-S)
- Hunt, D., & Tucker, M. E. (1995). Stranded parasequences and the forced regressive wedge systems tract: Deposition during base-level fall – Reply. *Sedimentary Geology*, *95*(1-2), 147–160. [https://doi.org/10.1016/0037-0738\(94\)00123-C](https://doi.org/10.1016/0037-0738(94)00123-C)
- Jerolmack, D. J., & Swenson, J. B. (2007). Scaling relationships and evolution of distributary networks on wave-influenced deltas. *Geophysical Research Letters*, *34*, L23402. <https://doi.org/10.1029/2007GL031823>
- Kisucki, M. J. (1987). Sedimentology, stratigraphy and paleogeography of the lower Cretaceous Mesa Rica delta system, Tatum Basin, east-central New Mexico. MS thesis, University of New Mexico, Albuquerque.
- Korus, J. T., & Fielding, C. R. (2017). Hierarchical architecture of sequences and bounding surfaces in a depositional-dip transect of the fluvio-deltaic Ferron Sandstone (Turonian), southeastern Utah, USA. *Journal of Sedimentary Research*, *87*, 897–920. <https://doi.org/10.2110/jsr.2017.50>
- Lamb, M. P., Nittrouer, J. A., Mohrig, D., & Shaw, J. (2012). Backwater and river plume controls on scour upstream of river mouths: Implications for fluvio-deltaic morphodynamics. *Journal of Geophysical Research*, *117*, F01002. <https://doi.org/10.1029/2011JF002079>
- Leclair, S. F., & Bridge, J. S. (2001). Quantitative interpretation of sedimentary structures formed by river dunes. *Journal of Sedimentary Research*, *71*, 713–716. <https://doi.org/10.1306/2DC40962-0E47-11D7-8643000102C1865D>
- Lin, W., & Bhattacharya, J. P. (2017). Estimation of source-to-sink mass balance by a fulcrum approach using channel paleohydrologic parameters of the Cretaceous Dunvegan Formation, Canada. *Journal of Sedimentary Research*, *87*, 97–116. <https://doi.org/10.2110/jsr.2017.1>
- MacEachern, J. A., & Bann, K. L. (2008). The role of ichnology in refining shallow marine facies models. In G. J. Hampson, R. J. Steel, P. M. Burgess, & R. W. Dalrymple (Eds.), *Recent advances in models of siliciclastic shallow-marine stratigraphy* (pp. 73–116). SEPM. <https://doi.org/doi:10.2110/pec.08.90.0073>
- MacEachern, J. A., Bann, K. L., Bhattacharya, J. P., & Howell, Jr., C. D. (2005). Ichnology of deltas; organism responses to the dynamic interplay of rivers, waves, storms, and tides. *Special Publication – Society for Sedimentary Geology*, *83*, 49–85.
- MacKenzie, D. B., & Poole, D. M. (1962). Provenance of Dakota group sandstones of the western interior. *Wyoming Geological Association*. [https://doi.org/10.1130/0016-7606\(1948\)59\[463:COTGR\]2.0.CO;2](https://doi.org/10.1130/0016-7606(1948)59[463:COTGR]2.0.CO;2)
- Mackin, J. H. (1948). Concept of the graded river. *Geological Society of America Bulletin*, *59*, 463–512. [https://doi.org/10.1130/0016-7606\(1948\)59\[463:COTGR\]2.0.CO;2](https://doi.org/10.1130/0016-7606(1948)59[463:COTGR]2.0.CO;2)
- Madof, A. S., Harris, A. D., & Connell, S. D. (2016). Nearshore along-strike variability: Is the concept of the systems tract unhinged? *Geology*, *44*, 315–318. <https://doi.org/10.1130/G37613.1>
- Martin, J., Cantelli, A., Paola, C., Blum, M., & Wolinsky, M. (2011). Quantitative modeling of the evolution and geometry of incised valleys. *Journal of Sedimentary Research*, *81*, 64–79. <https://doi.org/10.2110/jsr.2011.5>
- Martin, J., Fernandes, A. M., Pickering, J., Howes, N., Mann, S., & McNeil, K. (2018). The stratigraphically preserved signature of persistent backwater dynamics in a large paleodelta system: The Mungaroo Formation, North West Shelf, Australia. *Journal of Sedimentary Research*, *88*, 850–872. <https://doi.org/10.2110/jsr.2018.38>
- Martin, J., Paola, C., Abreu, V., Neal, J., & Sheets, B. (2009). Sequence stratigraphy of experimental strata under known conditions of differential subsidence and variable base level. *AAPG Bulletin*, *93*, 503–533. <https://doi.org/10.1306/12110808057>
- Martinsen, O. J., & Helland-Hansen, W. (1995). Strike variability of clastic depositional systems: Does it matter for sequence-stratigraphic analysis? *Geology*, *23*, 439–442. [https://doi.org/10.1130/0091-7613\(1995\)023<0439:SVOCDS>2.3.CO;2](https://doi.org/10.1130/0091-7613(1995)023<0439:SVOCDS>2.3.CO;2)
- Miall, A. D. (2015). Updating uniformitarianism: Stratigraphy as just a set of “frozen accidents”. *Geological Society, London, Special Publications*, *404*, 11–36. <https://doi.org/10.1144/SP404.4>
- Morshedian, A., MacEachern, J. A., Dashtgard, S. E., Bann, K. L., & Pemberton, S. G. (2019). Systems tracts and their bounding surfaces in the low-accommodation Upper Mannville group, Saskatchewan, Canada. *Marine and Petroleum Geology*, *110*, 35–54. <https://doi.org/10.1016/j.marpetgeo.2019.07.011>
- Nittrouer, J. A. (2013). Backwater hydrodynamics and sediment transport in the lowermost Mississippi River Delta: Implications for the development of fluvial-deltaic landforms in a large lowland river. In F. J. Young, G. M. E. Perillo, H. Aksoy, J. Bogen, A. Gelfan, G. Mahé, P. Marsh, & H. H. G. Savenije (Eds.), *Deltas: Landforms, Ecosystems, and Human Activities* (pp. 48–61). Gothenburg, Sweden: International Association of Hydrological Sciences Publication.
- Nittrouer, J. A., Shaw, J., Lamb, M. P., & Mohrig, D. (2012). Spatial and temporal trends for water-flow velocity and bed-material sediment transport in the lower Mississippi River. *Geological Society of America Bulletin*, *124*, 400–414. <https://doi.org/10.1130/B30497.1>
- Oboh-Ikuenobe, F. E., Holbrook, J. M., Scott, R. W., Akins, S. L., Evetts, M. J., Benson, D. G., & Pratt, L. M. (2008). Anatomy of epicontinental flooding: Late Albian-Early Cenomanian of the southern U.S. Western Interior Basin. In B. R. Pratt & C. Holmden (Eds.), *Dynamics of epeiric seas. Geological association of Canada, special paper* (pp. 201–227). [https://doi.org/10.1016/0016-7037\(86\)90064-5](https://doi.org/10.1016/0016-7037(86)90064-5)
- Olariu, C., & Bhattacharya, J. P. (2006). Terminal distributary channels and delta front architecture of river-dominated delta systems. *Journal of Sedimentary Research*, *76*, 212–233. <https://doi.org/10.2110/jsr.2006.026>
- Paola, C., Ganti, V., Mohrig, D., Runkel, A. C., & Straub, K. M. (2018). Time not our time: Physical controls on the preservation and measurement of geologic time. *Annual Review of Earth and Planetary Sciences*, *46*, 409–438. <https://doi.org/10.1146/annurev-earth-082517-010129>
- Paola, C., & Mohrig, D. (1996). Palaeohydraulics revisited: Palaeoslope estimation in coarse-grained braided rivers. *Basin Research*, *8*, 243–254. <https://doi.org/10.1046/j.1365-2117.1996.00253.x>
- Pattison, S. A. J. (2018). Rethinking the incised-valley fill paradigm for Campanian Book Cliffs strata, Utah-Colorado, U.S.A.: Evidence for discrete parasequence-scale, shoreface-incised channel fills. *Journal of Sedimentary Research*, *88*, 1381–1412. <https://doi.org/10.2110/jsr.2018.72>
- Pattison, S. A. J. (2019). High resolution linkage of channel-coastal plain and shallow marine facies belts, Desert Member to Lower Castlegate Sandstone stratigraphic interval, Book Cliffs, Utah-Colorado, USA. *GSA Bulletin*, *131*, 1643–1672. <https://doi.org/10.1130/B35094.1>

- Pecha, M. E., Gehrels, G. E., Karlstrom, K. E., Dickinson, W. R., Donahue, M. S., Gonzales, D. A., & Blum, M. D. (2018). Provenance of cretaceous through Eocene strata of the four corners region: Insights from detrital zircons in the San Juan Basin, New Mexico and Colorado. *Geosphere*, *14*, 785–811. <https://doi.org/10.1130/GES01485.1>
- Posamentier, H. W., Allen, G. P., James, D. P., & Tesson, M. (1992). Forced regressions in a sequence stratigraphic framework: Concepts, examples, and exploration significance. *AAPG Bulletin*, *76*, 1687–1709.
- Posamentier, H. W., Jervey, M. T., & Vail, P. R. (1988). Eustatic controls on clastic deposition I – Conceptual framework. In C. K. Wilgus, B. S. Hastings, C. G. S. C. Kendall, H. W. Posamentier, C. A. Ross, & J. C. Van Wagoner (Eds.), *Sea level changes – An integrated approach* (Vol. 42, pp. 110–124). Tulsa, Oklahoma: SEPM Special Publication.
- Posamentier, H. W., & Vail, P. R. (1988). Eustatic controls on clastic deposition II – Sequence and systems tract models. In C. K. Wilgus, B. S. Hastings, C. G. S. C. Kendall, H. W. Posamentier, C. A. Ross, & J. C. Van Wagoner (Eds.), *Sea level changes – An integrated approach* (Vol. 42, pp. 125–154). Tulsa, Oklahoma: SEPM Special Publication.
- Quirk, D. G. (1996). ‘Base profile’: A unifying concept in alluvial sequence stratigraphy. *Geological Society, London, Special Publications*, *104*, 37–49. <https://doi.org/10.1144/GSL.SP.1996.104.01.04>
- Scott, R. W. (1974). Bay and shoreface benthic communities in the Lower Cretaceous. *Lethaia*, *7*, 315–330.
- Scott, R. W., Holbrook, J. M., Oboh-Ikuenobe, F. E., Evetts, M. J., Benson, D. G., & Kues, B. S. (2004). Middle Cretaceous stratigraphy, southern Western Interior Seaway, New Mexico and Oklahoma. *Rocky Mountain Association of Geologists*, *41*, 33–61.
- Scott, R. W., Oboh-Ikuenobe, F. E., Benson, D. G., Holbrook, J. M., & Alnahwi, A. (2018). Cenomanian-Turonian flooding cycles: U.S. Gulf Coast and Western interior. *Cretaceous Research*, *89*, 191–210. <https://doi.org/10.1016/J.CRETRES.2018.03.027>
- Snow, R. S., & Slingerland, R. L. (1987). Mathematical modeling of graded river profiles. *Journal of Geology*, *95*, 15–33. <https://doi.org/10.1086/629104>
- Straub, K. M., & Esposito, C. R. (2013). Influence of water and sediment supply on the stratigraphic record of alluvial fans and deltas: Process controls on stratigraphic completeness. *Journal of Geophysical Research: Earth Surface*, *118*, 625–637. <https://doi.org/10.1002/jgrf.20061>
- Strong, N., & Paola, C. (2008). Valleys that never were: Time surfaces versus stratigraphic surfaces. *Journal of Sedimentary Research*, *78*, 579–593. <https://doi.org/10.2110/jsr.2008.059>
- Suleiman, A. S., & Keller, G. R. (1985). A geophysical study of basement structure in northeastern New Mexico. In S. G. Lucas & J. Zidek (Eds.), *Santa Rosa - Tucumcari Region* (pp. 153–159). Sorocco, New Mexico: New Mexico Geological Society, 36th field conference.
- Talling, P. J. (1998). How and where do incised valleys form if sea level remains above the shelf edge? *Geology*, *26*, 87–90.
- Trampus, S. M., Huzurbazar, S., & McElroy, B. (2014). Empirical assessment of theory for bankfull characteristics of alluvial channels. *Water Resources Research*, *50*, 9211–9220. <https://doi.org/10.1002/2014WR015597>
- Trower, E. J., Ganti, V., Fischer, W. W., & Lamb, M. P. (2018). Erosional surfaces in the Upper Cretaceous Castlegate Sandstone (Utah, USA): Sequence boundaries or autogenic scour from backwater hydrodynamics? *Geology*, *46*, 707–710. <https://doi.org/10.1130/G40273.1>
- Van Wagoner, J. C. (1995). Sequence stratigraphy and marine to nonmarine facies architecture of foreland basin strata, Book Cliffs, Utah, USA. In Van Wagoner, J. C. & G. T. Bertram (Eds.), *Sequence stratigraphy of foreland basin deposits: Outcrop and subsurface examples from the cretaceous of North America* (Vol. 64, pp. 137–223). Tulsa, Oklahoma, USA: AAPG Memoires.
- Van Wagoner, J. C., Posamentier, H. W., Mitchum, R. M., Vail, P. R., Sarg, J. F., Loutit, T. S., & Hardenbol, J. (1988). An overview of the fundamentals of sequence stratigraphy and key definitions. In C. K. Wilgus, B. S. Hastings, C. G. Kendall, C. St. H. W. Posamentier, C. A. Ross, & J. C. Van Wagoner (Eds.), *Sea-level changes: An integrated approach: Tulsa, Oklahoma* (pp. 39–45). SEPM Special Publication. <https://doi.org/10.2110/pec.88.01.0039>
- Van Yperen, A. E., Holbrook, J. M., Poyatos-Moré, M., & Midtkandal, I. (2019). Coalesced delta-front sheet-like sandstone bodies from highly avulsive distributary channels: The low-accommodation Mesa Rica Sandstone (Dakota Group, New Mexico, U.S.A.). *Journal of Sedimentary Research*, *89*, 654–678. <https://doi.org/10.2110/jsr.2019.27>
- Van Yperen, A. E., Line, L. H., Holbrook, J. M., Poyatos-Moré, M., & Midtkandal, I. (2019). Revised stratigraphic relationships of the Dakota Group in the Tucumcari Basin, San Miguel County, New Mexico, USA. In F. Ramos, M. J. Zimmerer, K. Zeigler, & D. Ulmer-Scholle (Eds.), *Geology of the Raton-clayton area*. (pp. 89–100). Socorro, New Mexico: New Mexico geological society guidebook, 70th field conference.
- Van Yperen, A. E., Poyatos-Moré, M., Holbrook, J. M., & Midtkandal, I. (2020). Internal mouth bar variability and preservation of interflood beds in low-accommodation proximal deltaic settings (Cretaceous Dakota Group, New Mexico, USA). *The Depositional Record*. <https://doi.org/10.1002/dep2.100>
- Waage, K. M. (1955). Dakota group in northern front range foothills, Colorado. *U.S. Geological Survey Professional Paper*, *274-B*, B15–B51.
- Wescott, W. A. (1993). Geomorphic thresholds and complex response of fluvial systems – Some implications for sequence stratigraphy. *AAPG Bulletin*, *77*, 1208–1218.
- Yalin, M. S. (1992). *River mechanics*. Oxford, UK: Pergamon Press. <https://doi.org/10.1016/C2009-0-06841-X>
- Zheng, S., Edmonds, D. A., Wu, B., & Han, S. (2019). Backwater controls on the evolution and avulsion of the Qingshuigou channel on the Yellow River Delta. *Geomorphology*, *333*, 137–151. <https://doi.org/10.1016/j.geomorph.2019.02.032>
- Zuchuat, V., Midtkandal, I., Poyatos-Moré, M., Da Costa, S., Brooks, H. L., Halvorsen, K., ... Braathen, A. (2019). Composite and diachronous stratigraphic surfaces in low-gradient, transitional settings: The J-3 “unconformity” and the Curtis Formation, east-central Utah, U.S.A. *Journal of Sedimentary Research*, *89*, 1075–1095. <https://doi.org/10.2110/jsr.2019.56>

SUPPORTING INFORMATION

Additional Supporting Information may be found online in the Supporting Information section.

How to cite this article: van Yperen AE, Holbrook JM, Poyatos-Moré M, Myers C, Midtkandal I. Low-accommodation and backwater effects on sequence stratigraphic surfaces and depositional architecture of fluvio-deltaic settings (Cretaceous Mesa Rica Sandstone, Dakota Group, USA). *Basin Res.* 2020;00:1–31. <https://doi.org/10.1111/bre.12483>